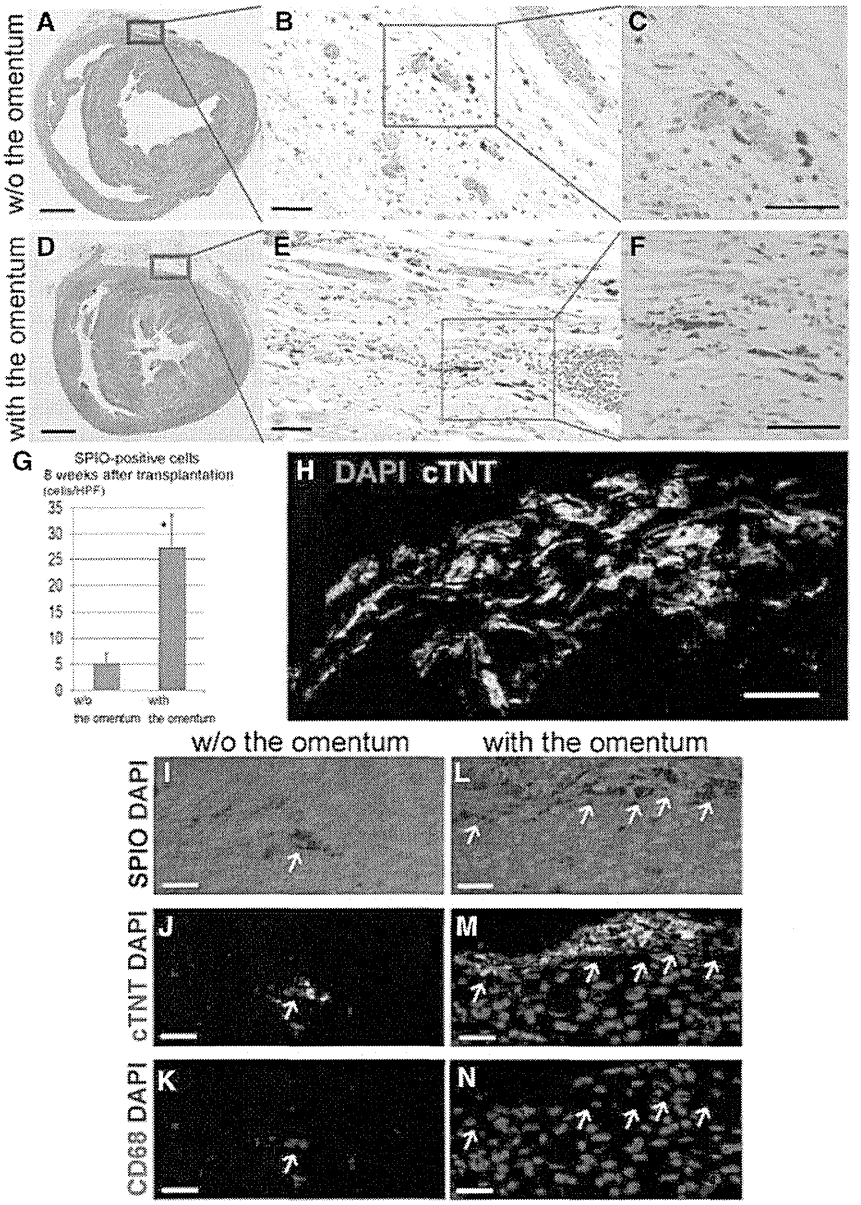

Figure 4. Human induced pluripotent stem cell–derived cardiomyocytes (hiPS-CMs) after transplantation. Macroscopic images of the whole heart by hematoxylin–eosin staining at the mid level in the mini-pig without (**A**) or with (**D**) the omentum; scale bar, 1 cm in **A** and **D**. Cells containing iron, indicative of superparamagnetic iron oxide (SPIO)–labeled hiPS-CMs, were detected by Prussian blue staining of sections of mini-pigs without (**B** and **C**) or with (**E** and **F**) the omentum at the transplanted area; scale bar, 50 μm in **B**, **C**, **E**, and **F**. **G**, The density of SPIO-positive cells in the transplanted site was semiquantitatively assessed at 8 weeks after treatment. **P*<0.0001 vs without the omentum. **H**, In the transplanted regions of mini-pigs with the omentum, cardiac troponin T (cTNT)–positive cells were also demonstrated by immunohistolabeling (green). The cell nuclei were counterstained with 4′,6-diamidino-2-phenylindole (DAPI; blue); scale bar, 50 μm in **H**. **I–N**, In the transplanted regions of mini-pigs, SPIO particles were visualized by differential interference contrast (DIC), and grafted hiPS-CMs, which were double-positive for cTNT (green) and SPIO (DIC) and negative for CD68 (red), were indentified by immunohistolabeling. The cell nuclei were counterstained with DAPI (blue). Arrows indicate SPIO particles, referred to DIC images in **I** and **L**; scale bar, 20 μm in **I–N**.

our hiPS-CM preparation protocols referred to in these studies to yield the amount of contracting hiPS-CMs contributing to the mechanical function of the injured heart. In addition, we previously demonstrated that maturation of iPS-CMs progressed after iPS-CMs were transplanted in nude rat heart.[28] Therefore, we also expect that improving environments after cell transplantation, such as avoiding delivered cell ischemia, inflammation, and immunogenic rejection, will promote in vivo differentiation of iPS-CMs and their therapeutic effects. The combination of hiPS-CM sheets and the omentum is a promising delivery method to differentiate hiPS-CMs in vivo, because the omentum at least prevents cell ischemia after transplantation and provides better environments.

The cause of reduction in the graft size during the 8 weeks after the cell-sheet transplantation in both groups was not fully addressed in this study. However, one may consider that this reduction was caused by host immune rejection. We used a combined 3 immunosuppressant regimen, consisting of tacrolimus, mycophenolate mofetil, and corticosteroid, because our experiment was a xenotransplantation model, in which human tissue–derived cells were transplanted in a porcine. In addition, mesenchymal stem cells, which have the potential to induce immunologic tolerance,[29] were involved in creating hiPS-CM cell sheets, and recent studies have reported that the omentum has not only angiogenic cytokines and growth factors but also anti-inflammatory properties and thus can facilitate tissue healing of injured tissue or organs.[30] With our cell delivery method that combines the cell-sheet method with the pedicled omental flap, the 3-drug immunosuppressant regimen, and a mixture of mesenchymal stem cells, it would be difficult to permanently maintain a large number of delivered cells in this xenotransplantation model. Future clinical study of hiPS-CM transplantation for treating heart disease might be performed as allogeneic transplantation.[31] Further studies related to immunologic tolerance are needed to maintain the delivered cells long-term or permanently in this treatment.

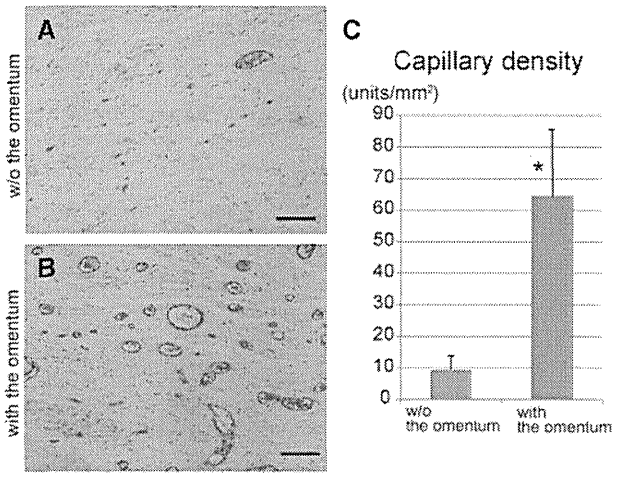

Figure 5. Capillary density in the transplanted area. Photomicrographs of immunostaining for von Willebrand factor are shown in **A** and **B**; scale bar, 50 μm. **C**, The capillary density in the transplanted area was significantly greater in the mini-pigs with the omentum than in those without it. *P<0.0001 vs without the omentum.

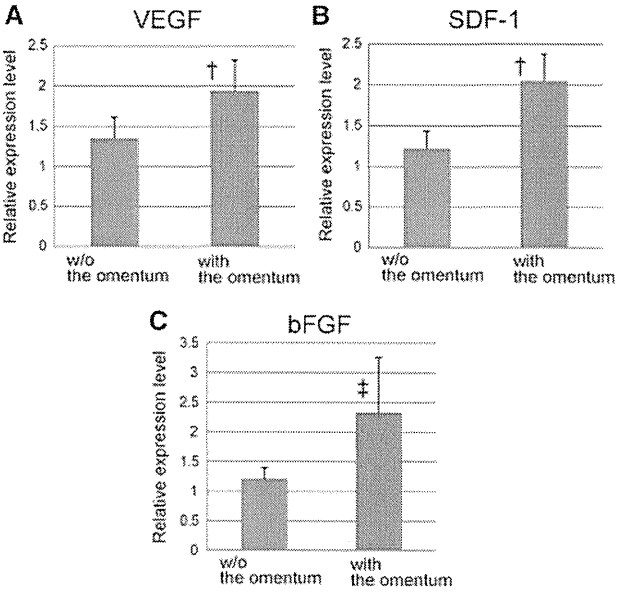

Figure 6. Angiogenesis-related mRNA expression in the transplanted area, as measured by real-time polymerase chain reaction. Relative expression of angiogenesis-related factors at the transplanted area was significantly greater in mini-pigs with the omentum than in those without it (**A**, vascular endothelial growth factor [VEGF], †P<0.05; **B**, stromal-derived factor [SDF]-1, †P<0.05; **C**, basic fibroblast growth factor [bFGF], ‡P<0.01 vs without the omentum).

In addition, more importantly, hiPS-CM cell sheets were transplanted over the normal epicardium, in which the tissue structure is well organized. New vascular network formation between the native myocardium and the transplanted cell sheets is thus insufficient to support the survival of the transplanted cells, leading to reduction of surviving transplanted cells long-term. In the clinical scenario, however, cell sheets will be transplanted over the diseased heart surface, in which epicardial structure is impaired. Conditions of the host myocardium possibly influence the survival of the transplanted cells. Our results indicate that transplanted cell sheets may provide sufficient blood supply, not from the host myocardium but from the omentum tissue. Thus, we consider that the omentum flap technique could provide a well-organized vascular network, regardless of conditions of the host myocardium, to enhance the survival of the transplanted cells. Further studies are needed to explore the mechanisms underlying integration of the transplanted cells sheets into the heart and to develop methods to enhance the survival and functionality of the transplanted cells.

Cardiac tissue engineering is another strategy that uses stem cells for the treatment of heart failure. One of the major challenges of in vitro engineering techniques is to overcome the limited thickness of the construct because the maximum oxygen diffusion is limited to ≈200 μm^2. A few recent methodologies have successfully yielded thicker engineered cardiac tissues. Cardiomyocytes in the Matrigel matrix were implanted with an arteriovenous blood vessel loop in vivo, and spontaneously contracting, thick, 3-dimensional constructs with extensive vascularization were thus attained.[32] The cell-sheet method, which is a scaffold-free system, is also an in vitro engineering technique. A cell sheet, itself, has a potential to induce angiogenesis quickly after implantation, and cell-dense 1-mm thick cardiac tissue was developed by repeated transplantation of triple-layered rat neonatal cardiac cell sheets.[33] This cardiac graft generated by this method, however, would be limited in use as a graft transplanted to the heart because of the lack of responsible large arteries and veins that can be revascularized after transplantation to the heart. In the present study, we used the omentum as a blood supply source after cell transplantation and demonstrated that the omentum enhanced angiogenesis and survival of the delivered cells. In addition, the omentum can easily be handled and mobilized, preserving its vascular network. The omentum, therefore, is a promising tool for in vivo vascularization in cardiac tissue engineering, although further studies with technological development would be needed for this strategy.

In conclusion, covering of the omentum flap over the transplanted hiPS-CM cell sheets on the myocardium effectively promoted angiogenesis, leading to enhanced survival of the hiPS-CMs. These results warrant further investigations as a clinically relevant strategy to enhance hiPS-CM transplantation therapy for heart failure.

Acknowledgments

We thank Shigeru Matsumi, Yuka Fujiwara, Hiromi Nishinaka, and Akima Harada for their excellent technical assistance.

Sources of Funding

This work was supported by the Japan Society for the Promotion of Science Core-to-Core Program and the Highway Program for the Realization of Regenerative Medicine of the Japanese Ministry of Education Sports, Science, and Technology.

Disclosures

Dr Shimizu is a consultant for CellSeed, Inc. Dr Okano is an Advisory Board Member in CellSeed, Inc, and an inventor/developer designated on the patent for temperature -responsive culture surfaces. The other authors report no conflicts.

References

1. Menasche P. Cardiac cell therapy: lessons from clinical trials. *J Mol Cell Cardiol*. 2011;50:258–265.
2. Hsiao LC, Carr C, Chang KC, Lin SZ, Clarke K. Stem cell-based therapy for ischemic heart disease. *Cell Transplant*. 2013;22:663–675.
3. Chimenti I, Smith RR, Li TS, Gerstenblith G, Messina E, Giacomello A, Marbán E. Relative roles of direct regeneration versus paracrine effects of human cardiosphere-derived cells transplanted into infarcted mice. *Circ Res*. 2010;106:971–980.
4. Tang XL, Rokosh G, Sanganalmath SK, Yuan F, Sato H, Mu J, Dai S, Li C, Chen N, Peng Y, Dawn B, Hunt G, Leri A, Kajstura J, Tiwari S, Shirk G, Anversa P, Bolli R. Intracoronary administration of cardiac progenitor cells alleviates left ventricular dysfunction in rats with a 30-day-old infarction. *Circulation*. 2010;121:293–305.
5. Takahashi K, Tanabe K, Ohnuki M, Narita M, Ichisaka T, Tomoda K, Yamanaka S. Induction of pluripotent stem cells from adult human fibroblasts by defined factors. *Cell*. 2007;131:861–872.
6. Yu J, Vodyanik MA, Smuga-Otto K, Antosiewicz-Bourget J, Frane JL, Tian S, Nie J, Jonsdottir GA, Ruotti V, Stewart R, Slukvin II, Thomson JA. Induced pluripotent stem cell lines derived from human somatic cells. *Science*. 2007;318:1917–1920.
7. Yoshida Y, Yamanaka S. iPS cells: a source of cardiac regeneration. *J Mol Cell Cardiol*. 2011;50:327–332.
8. Shimizu T, Yamato M, Isoi Y, Akutsu T, Setomaru T, Abe K, Kikuchi A, Umezu M, Okano T. Fabrication of pulsatile cardiac tissue grafts using a novel 3-dimensional cell sheet manipulation technique and temperature-responsive cell culture surfaces. *Circ Res*. 2002;90:e40.
9. Zvibel I, Smets F, Soriano H. Anoikis: roadblock to cell transplantation? *Cell Transplant*. 2002;11:621–630.
10. Memon IA, Sawa Y, Fukushima N, Matsumiya G, Miyagawa S, Taketani S, Sakakida SK, Kondoh H, Aleshin AN, Shimizu T, Okano T, Matsuda H. Repair of impaired myocardium by means of implantation of engineered autologous myoblast sheets. *J Thorac Cardiovasc Surg*. 2005;130:1333–1341.
11. Sekine H, Shimizu T, Dobashi I, Matsuura K, Hagiwara N, Takahashi M, Kobayashi E, Yamato M, Okano T. Cardiac cell sheet transplantation improves damaged heart function via superior cell survival in comparison with dissociated cell injection. *Tissue Eng Part A*. 2011;17:2973–2980.
12. Sawa Y, Miyagawa S, Sakaguchi T, Fujita T, Matsuyama A, Saito A, Shimizu T, Okano T. Tissue engineered myoblast sheets improved cardiac function sufficiently to discontinue LVAS in a patient with DCM: report of a case. *Surg Today*. 2012;42:181–184.
13. Kawamura M, Miyagawa S, Miki K, Saito A, Fukushima S, Higuchi T, Kawamura T, Kuratani T, Daimon T, Shimizu T, Okano T, Sawa Y. Sheets in a porcine ischemic cardiomyopathy model. *Circulation*. 2012;126:S29–S37.
14. O'Shaugnessy L. Surgical treatment of cardiac ischemia. *Lancet*. 1937;232:185–94.
15. Bigelow WG, Basian H, Trusler GA. Internal mammary artery implantation for coronary heart disease. A clinical follow-up study on to eight years after operation. *J Thorac Cardiovasc Surg*. 1963;45:67–79.
16. Aldridge HE, Macgregor DC, Lansdown EL, Bigelow WG. Internal mammary artery implantation for the relief of angina pectoris: a follow-up study of 77 patients for up to 13 years. *Can Med Assoc J*. 1968;98:194–198.
17. Shrager JB, Wain JC, Wright CD, Donahue DM, Vlahakes GJ, Moncure AC, Grillo HC, Mathisen DJ. Omentum is highly effective in the management of complex cardiothoracic surgical problems. *J Thorac Cardiovasc Surg*. 2003;125:526–532.
18. Takaba K, Jiang C, Nemoto S, Saji Y, Ikeda T, Urayama S, Azuma T, Hokugo A, Tsutsumi S, Tabata Y, Komeda M. A combination of omental flap and growth factor therapy induces arteriogenesis and increases myocardial perfusion in chronic myocardial ischemia: evolving concept of biologic coronary artery bypass grafting. *J Thorac Cardiovasc Surg*. 2006;132:891–899.
19. Shudo Y, Miyagawa S, Fukushima S, Saito A, Shimizu T, Okano T, Sawa Y. Novel regenerative therapy using cell-sheet covered with omentum flap delivers a huge number of cells in a porcine myocardial infarction model. *J Thorac Cardiovasc Surg*. 2011;142:1188–1196.
20. Toyoda K, Tooyama I, Kato M, Sato H, Morikawa S, Hisa Y, Inubushi T. Effective magnetic labeling of transplanted cells with HVJ-E for magnetic resonance imaging. *Neuroreport*. 2004;15:589–593.
21. Miyoshi S, Flexman JA, Cross DJ, Maravilla KR, Kim Y, Anzai Y, Oshima J, Minoshima S. Transfection of neuroprogenitor cells with iron nanoparticles for magnetic resonance imaging tracking: cell viability, differentiation, and intracellular localization. *Mol Imaging Biol*. 2005;7:286–295.
22. Kraitchman DL, Heldman AW, Atalar E, Amado LC, Martin BJ, Pittenger MF, Hare JM, Bulte JW. *In vivo* magnetic resonance imaging of mesenchymal stem cells in myocardial infarction. *Circulation*. 2003;107:2290–2293.
23. Takehara N, Tsutsumi Y, Tateishi K, Ogata T, Tanaka H, Ueyama T, Takahashi T, Takamatsu T, Fukushima M, Komeda M, Yamagishi M, Yaku H, Tabata Y, Matsubara H, Oh H. Controlled delivery of basic fibroblast growth factor promotes human cardiosphere-derived cell engraftment to enhance cardiac repair for chronic myocardial infarction. *J Am Coll Cardiol*. 2008;52:1858–1865.
24. Mangi AA, Noiseux N, Kong D, He H, Rezvani M, Ingwall JS, Dzau VJ. Mesenchymal stem cells modified with Akt prevent remodeling and restore performance of infarcted hearts. *Nat Med*. 2003;9:1195–1201.
25. Li W, Ma N, Ong LL, Nesselmann C, Klopsch C, Ladilov Y, Furlani D, Piechaczek C, Moebius JM, Lützow K, Lendlein A, Stamm C, Li RK, Steinhoff G. Bcl-2 engineered MSCs inhibited apoptosis and improved heart function. *Stem Cells*. 2007;25:2118–2127.
26. Tulloch NL, Muskheli V, Razumova MV, Korte FS, Regnier M, Hauch KD, Pabon L, Reinecke H, Murry CE. Growth of engineered human myocardium with mechanical loading and vascular coculture. *Circ Res*. 2011;109:47–59.
27. Matsuura K, Wada M, Shimizu T, Haraguchi Y, Sato F, Sugiyama K, Konishi K, Shiba Y, Ichikawa H, Tachibana A, Ikeda U, Yamato M, Hagiwara N, Okano T. Creation of human cardiac cell sheets using pluripotent stem cells. *Biochem Biophys Res Commun*. 2012;425:321–327.
28. Yu T, Miyagawa S, Miki K, Saito A, Fukushima S, Higuchi T, Kawamura M, Kawamura T, Ito E, Kawaguchi N, Sawa Y, Matsuura N. *In vivo* differentiation of induced pluripotent stem cell-derived cardiomyocytes. *Circ J*. 2013;77:1297–1306.
29. Uccelli A, Moretta L, Pistoia V. Mesenchymal stem cells in health and disease. *Nat Rev Immunol*. 2008;8:726–736.
30. Chandra A, Srivastava RK, Kashyap MP, Kumar R, Srivastava RN, Pant AB. The anti-inflammatory and antibacterial basis of human omental defense: selective expression of cytokines and antimicrobial peptides. *PLoS One*. 2011;6:e20446.
31. Pearl JI, Lee AS, Leveson-Gower DB, Sun N, Ghosh Z, Lan F, Ransohoff J, Negrin RS, Davis MM, Wu JC. Short-term immunosuppression promotes engraftment of embryonic and induced pluripotent stem cells. *Cell Stem Cell*. 2011;8:309–317.
32. Morritt AN, Bortolotto SK, Dilley RJ, Han X, Kompa AR, McCombe D, Wright CE, Itescu S, Angus JA, Morrison WA. Cardiac tissue engineering in an *in vivo* vascularized chamber. *Circulation*. 2007;115:353–360.
33. Shimizu T, Sekine H, Yang J, Isoi Y, Yamato M, Kikuchi A, Kobayashi E, Okano T. Polysurgery of cell sheet grafts overcomes diffusion limits to produce thick, vascularized myocardial tissues. *FASEB J*. 2006;20:708–710.

PLOS ONE

Direct Induction of Chondrogenic Cells from Human Dermal Fibroblast Culture by Defined Factors

Hidetatsu Outani[1,2], Minoru Okada[1], Akihiro Yamashita[1], Kanako Nakagawa[2,3], Hideki Yoshikawa[2], Noriyuki Tsumaki[1,2,3]*

1 Department of Cell Growth and Differentiation, Center for iPS Cell Research and Application, Kyoto University, Kyoto, Japan, **2** Department of Orthopaedic Surgery, Osaka University Graduate School of Medicine, Suita, Osaka, Japan, **3** Japan Science and Technology Agency, CREST, Tokyo, Japan

Abstract

The repair of large cartilage defects with hyaline cartilage continues to be a challenging clinical issue. We recently reported that the forced expression of two reprogramming factors (c-Myc and Klf4) and one chondrogenic factor (SOX9) can induce chondrogenic cells from mouse dermal fibroblast culture without going through a pluripotent state. We here generated induced chondrogenic (iChon) cells from human dermal fibroblast (HDF) culture with the same factors. We developed a chondrocyte-specific *COL11A2* promoter/enhancer lentiviral reporter vector to select iChon cells. The human iChon cells expressed marker genes for chondrocytes but not fibroblasts, and were derived from non-chondrogenic *COL11A2*-negative cells. The human iChon cells formed cartilage but not tumors in nude mice. This approach could lead to the preparation of cartilage directly from skin in human, without going through pluripotent stem cells.

Citation: Outani H, Okada M, Yamashita A, Nakagawa K, Yoshikawa H, et al. (2013) Direct Induction of Chondrogenic Cells from Human Dermal Fibroblast Culture by Defined Factors. PLoS ONE 8(10): e77365. doi:10.1371/journal.pone.0077365

Editor: Dimas Tadeu Covas, University of Sao Paulo - USP, Brazil

Received February 20, 2013; **Accepted** September 2, 2013; **Published** October 16, 2013

Funding: This study was supported in part by Scientific Research Grants Nos. 18390415, 19659378 and 21390421 from MEXT and the JST, CREST. The funders had no role in study design, data collection and analysis, decision to publish, or preparation of the manuscript.

Competing Interests: The authors have declared that no competing interests exist.

* E-mail: ntsumaki@cira.kyoto-u.ac.jp

Introduction

Articular cartilage provides shock absorption and lubrication in diarthrodial joints. Articular cartilage is a hyaline cartilage which consists of chondrocytes and cartilage extracellular matrix composed of types II, IX and XI collagen molecules, proteoglycans, and other matrix proteins. Because hyaline cartilage has a poor intrinsic capacity for healing, the loss of cartilage due to trauma or degeneration caused by aging can result in debilitating conditions and osteoarthritis.

Cartilage damage sometimes heals with fibrocartilage, which differs from hyaline cartilage. Fibrocartilage is a type of scar tissue that expresses types I and II collagen; hyaline cartilage, in contrast, does not express type I collagen [1,2]. As the presence of type I collagen impairs the development of cartilage-specific matrix architecture and mechanical function, the repair of cartilage damage by fibrocartilage results in morbidity and functional impairment. Therefore, the goal for repair of cartilage injury is the regeneration of organized hyaline cartilage, rather than healing with fibrocartilage [3]. Although autologous chondrocyte implantation has been successfully performed, the indications are limited to a small size defect, because chondrocytes are limited in number, and because they de-differentiate into fibrochondrocytes during monolayer expansion in culture [4]. Defects larger than 4 cm^2 in size cannot be repaired because of the lack of a sufficient number of bona fide chondrocytes to fill the defect.

Sox9, Sox5 and Sox6 play important roles in the commitment of mesenchymal cells to the chondrocyte lineage. In mouse chimeras, $Sox9^{-/-}$ cells are excluded from the cartilage primordia throughout embryonic development [5,6]. Sox9, Sox5, and Sox6 activate the transcription of chondrocyte-marker genes by binding their enhancers [7–10]. It was reported that the forced expression of Sox5, Sox6 and Sox9 by adenoviral vectors in dermal fibroblasts causes the expression of their target gene, type II collagen [11]. However, the histology of pellet cultures of these cells appears to be fibrocartilaginous, suggesting that the fibroblastic characteristics of the cells persist. Therefore, the cells produced in that study may correspond to fibrocartilaginous cells, rather than hyaline cartilaginous cells. Although dermal fibroblasts represent a readily accessible cell source, their tendency for high expression of type I collagen is a large obstacle to the production of hyaline cartilage. To eliminate the fibroblastic characteristics of these cells, a cell reprogramming process may be necessary.

A large number of autologous hyaline chondrogenic cells may be obtained by generating iPS cells, followed by redifferentiation into a chondrocytic lineage in the future. However, transplantation of redifferentiated chondrocytes is associated with a risk of teratoma formation due to the possible presence of residual undifferentiated cells. Recently, we induced chondrogenic cells directly from adult mouse dermal fibroblast (MDF) culture by transduction of two reprogramming factors (c-Myc, Klf4) and SOX9 [12]. The induced chondrogenic cells formed histologically homogenous hyaline cartilage when injected into the subcutaneous spaces of nude mice. Time-lapse observations of MDF cultures prepared from Nanog-GFP transgenic mice [13] revealed that GFP was not expressed during the induction of chondrogenic cells by transduction of c-Myc, Klf4, and SOX9, proving that the cells do not transition through a pluripotent state during the direct induction of chondrogenic cells from MDFs [14]. Therefore, the

induced chondrogenic cells produced by this method are theoretically free from the risk of teratoma formation.

Future clinical application of this technique of regenerative medicine for articular cartilage diseases will require confirmation that chondrogenic cells can be directly induced from human dermal fibroblast culture. We here generated induced chondrogenic (iChon) cells from human dermal fibroblast (HDF) cultures. We employed nucleofection to misexpress Slc7a1, a receptor for retrovirus, followed by retroviral transduction of the same three factors, to cause the transformation of human dermal fibroblasts into chondrogenic lineage cells. We also developed a chondrocyte-specific *COL11A2* promoter/enhancer lentiviral reporter vector, to select human iChon cells. The human iChon cells expressed type II collagen, but not type I collagen. These human iChon cells generated stable homogenous hyaline cartilage-like tissue without tumor formation for at least 3 months in the subcutaneous spaces of nude mice.

Materials and Methods

Ethics Statement

All experiments were approved by our institutional animal committees, institutional biosafety committees, and institutional review boards of Osaka University and Kyoto University.

Lentiviral Vectors and Transduction

The pLenti6/UbC/mSlc7a1 (Addgene plasmid 17224) was a gift from S. Yamanaka (Center for iPS Cell Research and Application (CiRA), Kyoto University, Kyoto, Japan) [15].

For construction of chondrocyte-specific reporter vectors, the human sequences corresponding to the mouse *Col11a2* promoter and enhancer [16] were amplified by PCR. The human *COL11A2* enhancer was linked to the EGFP-IRES-Puro sequence in the pENTR5′ plasmid (Invitrogen) [12] to prepare pENTR1A-mcs/(EGFP-IresPuro-hInt) (P4-40). The human *COL11A2* promoter was cloned into the pENTR5′ plasmid (Invitrogen) to prepare pENTR5′-mcs/11P (P4-41). The lentiviral vector, pLe6Δ (P4-32) was prepared by deleting the PGKpromoter-EM7-Blastcidine sequence at KpnI sites from pLenti6.4/R4R2/V5-DEST (Invitrogen). pENTR1A-mcs/(EGFP-IresPuro-hInt) (P4-40) was recombined with pENTR5′-mcs/11P (P4-41) and pLe6Δ by the LR clonase II plus reaction (Invitrogen) to prepare pLe6Δ -hLP-mcs/(EGFP-IresPuro-hInt) (P4-42, *COL11a2*-reporter vector), respectively. Lentiviral transduction was performed following the manufacturer's instructions (Invitrogen).

Cell Culture

Human dermal fibroblasts (HDFs) prepared from neonatal foreskin were purchased from Kurabo (KF-4009). On arrival, the HDFs were thawed, and 5×10^5 cell were plated in a 10 cm dish in DMEM supplemented with 10% FBS. The next day, the cells were either untransduced, or were transduced with lentiviral *COL11A2*-reporter vectors overnight. The cells were subsequently split 1:5 into 10 cm dishes and stored in liquid nitrogen until use. Human chondrosarcoma (HCS-2/8) cells were cultured in DMEM supplemented with 10% FBS [17].

Chondrogenically Differentiated Human Bone Marrow Stem Cells

Human bone marrow stem cells (hBMSC) were purchased from Takara (PT-2501). On arrival of frozen stock of hBMSC, the cells were thawed and 3×10^5 cell were plated in a 10 cm dish in αMEM supplemented with 10% FBS. When the cells became confluent, the culture was passaged (P1). Expanded hBMSC (P2) were suspended at 3×10^5 cells/ml in αMEM containing 10% FBS, transferred into a 15-ml tube (Falcon), and centrifuged at 500 g for 5 min. The resulting cell pellet was incubated in a chondrogenic differentiation medium (purchased from Takara [PT-3003, PT-4124]) for 3 weeks, and the resulting cells were called chondrogenically differentiated human bone marrow stem cells (CD-hBMSC).

Nucleofection of *Slc7a1*

The *Slc7a1* sequence from pLenti6/UbC/mSlc7a1 (Addgene plasmid 17224) was cloned into pDONR221 (Invitrogen) by BP clonase (Invitrogen) to prepare pDONR221-mSlc7a1 (P8-63). pDONR221-mSlc7a1 (P8-63) was recombined with pCMVb-gw (P1-32) by the LR reaction (Invitrogen) to prepare pCMV-gw/mSlc7a1 (P9-75). pCMV-gw/mSlc7a1 (P9-75) was introduced into HDFs using nucleofection technology following the manufacturer's instructions (Amaxa).

Retroviral Vectors and Transduction

pMXs-c-MYC (Addgene plasmid 17220) and pMXs-KLF4 (Addgene plasmid 17219), were gifts from S. Yamanaka (Center for iPS Cell Research and Application (CiRA), Kyoto University, Kyoto, Japan) [15]. pMXs-hSOX9 was described previously [12]. Human SOX5 and SOX6 cDNAs were PCR amplified using specific primers (Table S3) and were cloned into pDONR222 vector (Invitrogen) to create pENTR-hSOX5 (P5-41) and pENTR-hSOX6 (P5-42). pENTR-hSOX5 (P5-41) or pENTR-hSOX6 (P5-42) were recombined with pMXs-gw by the LR reaction (Invitrogen) to prepare pMXs-gw/hSOX5 (P8-83) or pMXs-gw/hSOX5 (P8-84). A sequencing analysis showed the hSOX5 and hSOX6 sequences to be correct.

Retroviral transduction was performed as described previously [18]. The Plat-E cells were a gift from T. Kitamura (The Institute of Medical Science, The University of Tokyo, Tokyo, Japan) [19].

Equal amounts of supernatants containing each of the retroviruses were mixed and added to the HDF cultures. After a 16-h incubation in the virus-containing medium, each fibroblast culture in the 10 cm dishes was trypsinized and split 1:5 into new 10 cm dishes in fresh medium (DMEM supplemented with 10% FBS). The medium was changed every other day. In the cultures transduced with lentiviral *COL11A2*-reporter vectors, puromycin was added to the medium when GFP fluorescence was detected in some cells at around 7 days after retroviral transduction. At 21 days after retroviral transduction, dishes were subjected to alcian blue staining. The colony numbers were counted using the NIS Element software program (Nikon). We defined a colony as a cell cluster that was more than 0.5 mm in diameter. Other dishes were used for picking up colonies to generate induced chondrogenic cells.

Alcian Blue Staining

Cells were fixed with methanol at −20°C for 2 min, incubated with 0.1% alcian blue (Sigma) in 0.1 N HCl for 2 h at 25°C, and washed three times with distilled water.

Generation of Induced Chondrogenic Cell Lines

After setting up a sterile cylinder surrounding each colony, we harvested the cells by trypsinization, and replated them in 48 well dishes. After 6–10 days, the cells were replated in 24 well dishes. Then, cells were replated successively into 12 well, 6 well, 6 cm, and 10 cm dishes after culturing for them 3–14 days in each dish. We defined the stage of cells in 10 cm dishes as passage 6. The induced chondrogenic cells were cultured in DMEM containing

10% FBS in the presence of 1 μg/ml puromycin. Induced chondrogenic cells were passaged every 6 days. We initiated the growth curve analyses of induced chondrogenic cells at passage 11.

Genomic PCR Analysis

The iChon cells (passage 11) and HDFs (passage 3) were cultured in 60 mm dishes. After the cells reached confluence, the genomic DNA was extracted and subjected to PCR to amplify transgenes. For the control, a fragment of the GAPDH gene was amplified. The primers used are listed in Table S2.

RT-PCR and Real-time RT-PCR Analyses

After the iChon cells and HDFs cultured in 60 mm dishes reached confluence, the total RNA was extracted using RNeasy Mini Kits (Qiagen). The total RNAs prepared from the redifferentiated human fetal chondrocytes (HFC) were purchased from Cell Applications, Inc. (402RD-R10f). The total RNA was extracted from CD-hBMSCs. The total RNAs were digested with DNase to eliminate any contaminating genomic DNA. For RT-PCR analysis, 1 μg of total RNA was reverse transcribed into first-strand cDNA by using Superscript III Reverse Transcription (Invitrogen). PCR was performed with ExTaq (Takara). The primers used are listed in Tables S2 and S3. For real-time quantitative RT-PCR, 1 μg of total RNA was reverse transcribed into first-strand cDNA by using SuperScript III (Invitrogen) and an oligo(dT)$_{20}$ primer. The PCR amplification occurred in a reaction volume of 20 μl containing 2 μl of cDNA, 10 μl of SYBER PremixExTaq (Takara) and 7900HT (Applied Biosystems). The PCR primers used are listed in Table S3. The RNA expression levels were normalized to the level of *GAPDH* expression.

Determination of Karyotypes

iChon cells were subjected to karyotype analyses at Nihon Gene Laboratories (Japan).

Immunofluorescence Staining

The cells were cultured on culture slides, fixed in 4% paraformaldehyde and permeabilized with 0.5% Tween 20. The cells were then incubated with the primary antibodies listed in Supplemental Table S4. Immune complexes were detected by using the appropriate secondary antibodies conjugated to Alexa Fluor (Table S4).

Bisulfite Genomic Sequencing

Bisulfite treatment was performed by using the EpiTect Bisulfite kit (Qiagen) according to the manufacturer's instructions. The PCR primers used are listed in Table S3. Amplified products were cloned into the pMD20-T vector using a Mighty TA-cloning Kit (Takara). Twelve randomly selected clones were sequenced with the M13 primer, RV, and M13 primer, M4, for each gene.

Pellet Culture

Induced cells were suspended at 5×10^5 cells/ml in DMEM containing 10% FBS, transferred into a 15-ml tube (Falcon), and centrifuged at 500 g for 5 min. The resulting cell pellet was incubated in chondrogenic medium (DMEM, 10% FBS, TGF-β 10ng/ml, DEX 10^{-7} M, Ascorbic acid 50 μg/ml, Pyrubate 100 μg/ml and ITS 6.25 μg/ml) for 3 weeks.

Picrosirius Red Staining and Immunohistochemical Staining

Semi-serial histological sections were stained with picrosirius red using the Picrosisius red stain kit (Plysciences, Inc.) and immunostained with the primary and secondary antibodies listed in Table S4. For controls, sections from osteochodromas obtained at the time of surgery were used to test the anti-type I and anti-type II collagen antibodies.

In vivo Cartilaginous Tissue Formation in Nude Mice

The iChon cells were suspended at 1×10^7 cells/ml in DMEM containing 10% FBS. Then, 100 μl of the cell suspension was injected subcutaneously into the dorsal flank of 6-week-old female nude mice (BALB/cA Jcl-nu/nu). No carrier was used. The mice were sacrificed after 4, 8, 12 weeks, and the injected sites were dissected from the mice. Samples were fixed in 10% neutral buffered formalin, processed, and embedded in paraffin.

Implantation of Human iChon Cells into the Articular Cartilage Defects in Severe Combined Immunodeficiency (SCID) Rats

The skin and joint capsule of a knee joint in 6-week-old SCID rats (F344-Il2rgtm2kyo) [20] were opened. A drill hole with a diameter of 1 mm was created at the femoral groove. A pellet of 5×10^5 iChon cells was implanted into the hole, then the joint capsule and skin were closed. The rats were sacrificed four weeks later.

Culture of iChon Cells Under Osteogenic Conditions

A total of 2×10^5 iChon cells were plated in each well of a six well plate, and cultured in the osteogenic medium (α-MEM supplemented with 10% FBS, 10 mM β-glycerophosphate, 50 μg/ml ascorbic acid, and 10^{-7} M Dexamethasone in the absence or presence of various concentrations of BMP2). The medium was changed every other day. RNAs were extracted from the cells after 21 days of culture, and were subjected to a real-time RT-PCR expression analysis. As control, RNAs were extracted from subchondral bone samples collected from the tibia and femur at the time of surgery.

Implantation of iChon Cells into the Calvarial Defects of SCID Mice

The skin on the head of 5-week-old SCID mice (C.B-17/Icr-scid/scid Jcl) was incised, then a drill hole with a diameter of 1 mm was created at the calvarium. A pellet of 5×10^5 iChon cells was implanted into the hole, then the skin was closed. The mice were sacrificed three weeks later.

Statistical Analysis

The data are shown as averages and standard deviations. Two-tailed Student's *t*-tests were used to compare the data. P values <0.05 were considered to be statistically significant.

Results

The Generation of Human Induced Chondrogenic (iChon) Cells from HDFs by Transduction of c-MYC, KLF4 and SOX9

We first transduced neonatal foreskin HDF cells (Figure 1A, middle left panel) with lentiviral vectors bearing human c-MYC, KLF4 and SOX9, but failed to obtain cells with the polygonal morphology which is typical shape of cultured chondrocytes.

Therefore, we transduced HDFs with these factors following another previously described method using *Slc7a1* encoding a receptor for the retrovirus [15]. We tried to increase the titer of retroviral infection by transducing HDFs with *Slc7a1* using nucleofection technology to increase the expression levels of *Slc7a1*. Two days after the nucleofection of *Slc7a1*, we transduced the HDFs with retroviral c-MYC, KLF4 and SOX9 vectors. Five days after retroviral transduction, we detected polygonal cells in the HDF culture. The polygonal cells (Figure 1A, middle right panel) formed multiple layers at 14 days after transduction, giving rise to cell nodules (Figure 1A, bottom left panel) which is a characteristic of cultured primary chondrocytes [21]. The nodules were surrounded by cells that had the morphological appearance of fibroblasts. These nodules were specifically and intensely stained with alcian blue (Figure 1A, bottom right), suggesting the existence of acid glycosaminoglycans, which is an element of cartilage extracellular matrix. The surrounding cells that had the morphological appearance of fibroblasts were not stained with alcian blue. These results suggest that forced expression of c-MYC, KLF4 and SOX9 can produce induced chondrogenic (iChon) cells from human skin fibroblast cultures.

Selection of Human iChon Cells with a *COL11A2* Enhancer-based Lentiviral Reporter Vector

To remove fibroblastic cells and isolate homogenous polygonal-shaped iChon cell populations, we constructed a chondrocyte-specific reporter vector using EGFP and puromycin-resistant genes linked by the IRES sequence on the lentiviral vector. To obtain chondrocyte-specific expression, we employed promoter and enhancer sequences of the human α2(XI) collagen chain (*COL11A2*) gene (Figure S1A) that correspond to the mouse *Col11a2* promoter and enhancer, which direct chondrocyte-specific expression [16]. The *COL11A2*-reporter vector directed substantial GFP expression in human chondrosarcoma (HCS-2/8) cells [17] but not in HDFs (Figure S1B). We transduced the HDFs with lentiviral *COL11A2*-reporter vectors overnight, split them 1:5, and made a cell stock from these cells. The cell stock of HDFs transduced with reporters was thawed (day 0) and we nucleofected the cells with *Slc7a1* (day 2). We then replated 5×10^5 cells in a 10 cm dish (day 3) and transduced the cells with retroviral vectors bearing c-MYC, KLF4 and SOX9 (day 5) overnight. Immediately after retroviral transduction, the cells were split 1:5 in 10 cm dishes (day 6) (Figure 1B). Polygonal-shaped cells, which appeared 5 days after retroviral transduction with c-MYC, KLF4 and SOX9, started to show *COL11A2-GFP* fluorescence. Subsequently, the polygonal-shaped cells formed nodules. EGFP was expressed in the nodules, but not in the surrounding fibroblastic cells in the absence of puromycin (Figure 1B). The transduction of 5×10^5 HDFs with c-MYC, KLF4 and SOX9 resulted in the formation of 1200 nodules, which showed intense staining for alcian blue in the absence of puromycin (Figure 1C) in five 10 cm dishes. Therefore, the efficiency of the induction of alcian blue-positive cells was 0.24%. On the other hand, the transduction of HDFs with the control retroviral DsRed fluorescent protein vector resulted in neither nodule formation nor substantial alcian blue staining (Figure 1C). Because a combination of SOX9, SOX5 and SOX6 was previously reported to activate the expression of chondrocyte-markers in HDFs [11], we transduced HDFs with SOX9, SOX5 and SOX6. We confirmed that the SOX5, SOX6 and SOX9 proteins were expressed by immunoblot analyses (Figure S2). We found neither nodule formation nor any substantial alcian blue staining in the HDFs transduced with SOX9, SOX5 and SOX6 (Figure 1C). These results indicate that c-MYC and KLF4 play a critical role in the conversion from fibroblasts to chondrogenic cells by SOX9.

To isolate colonies, we started to add puromycin to the medium when GFP fluorescence was detected at 5–7 days after transduction with c-MYC, KLF4 and SOX9. The majority of fibroblastic cells and four-fifths of the polygonal-shaped cells died, leaving 267 surviving colonies, on average, in the culture in the presence of 1 μg/ml puromycin (Figure 1D). On average, 186 out of the 267 colonies were intensely stained with alcian blue and were composed of polygonal cells. The remaining 81 colonies were large and diffuse, as indicated by crystal violet staining, and were composed of fibroblastic cells. The transduction of HDFs with the control retroviral DsRed vector instead of c-MYC, KLF4 and SOX9 vectors produced 107 colonies in the presence of puromycin. These colonies were not stained with alcian blue (Figure 1D), and were composed of fibroblasts. These fibroblasts survived in the presence of puromycin, probably because of the aberrant expression of the lentiviral *COL11A2*-reporter vector. The transduction of HDFs with SOX9, SOX5 and SOX6 also produced 91 colonies in the presence of puromycin. These colonies did not stain for alcian blue (Figure 1D), and were composed of morphologically fibroblastic cells.

Therefore, the transduction of the lentiviral *COL11A2* reporter vector and selection with puromycin resulted in the formation of nodules as colonies, 70% of which were composed of polygonal-shaped cells. The colonies composed of polygonal cells were almost all intensely stained with alcian blue. We picked up colonies which were composed of polygonal-shaped cells, and added them in the wells of 48 well plates and expanded each cell line by replating them onto successively larger dishes. We established 15 clones which reached subconfluency in 10 cm dishes, and were subjected to the further analyses.

Characteristics of the iChon Cells

Isolated human iChon cells showed a polygonal morphology (Figure 2A). We found that all three (c-MYC, KLF4 and SOX9) transgenes were transduced into the genomic DNA (Figure S3A) and were expressed (Figure 2B) in iChon cells. These results suggest that retrovial transgenes were not silenced in iChon cells. A growth curve analysis showed that the proliferation rates of the established human iChon cell lines were lower than those of the parental HDFs (Figure 2C). A karyotype analysis showed that 20 out of 20 cells (iChon 87-18), 20 out of 20 cells (iChon 117-3) and 14 out of 20 cells (iChon 117-37) had normal karyotypes (Figure 2D and Figure S3B).

A real-time RT-PCR analysis showed that human iChon cells expressed neither *COL1A1* nor *COL1A2* mRNAs, which the parental HDFs expressed abundantly (Figure 3A). With regard to the control, redifferentiated human fetal chondrocytes (HFC) expressed both *COL1A1* and *COL1A2*, probably because fibroblasts had contaminated the cells during their collection, or because of dedifferentiation of chondrocytes during culture. On the other hand, the iChon cells expressed chondrocyte-specific marker genes, *COL2A1* and *ACAN*, whereas the HDFs did not. The iChon cell lines showed little expression levels of the hypertrophic chondrocyte marker *COL10A1* and terminally differentiated chondrocyte marker *MMP13* (Figure 3B). Regarding the control, we prepared chondrogenic cells by differentiation from human bone marrow stem cells. Chondrogenically differentiated human bone marrow stem cells (CD-hBMSCs) expressed *COL10A1* and *MMP13*. These expression patterns of iChon cells were maintained after passaging them (Figure S3C).

The bisulfate sequencing analysis revealed that the cytosine guanine (CpG) dinucleotides in the regulatory element of the

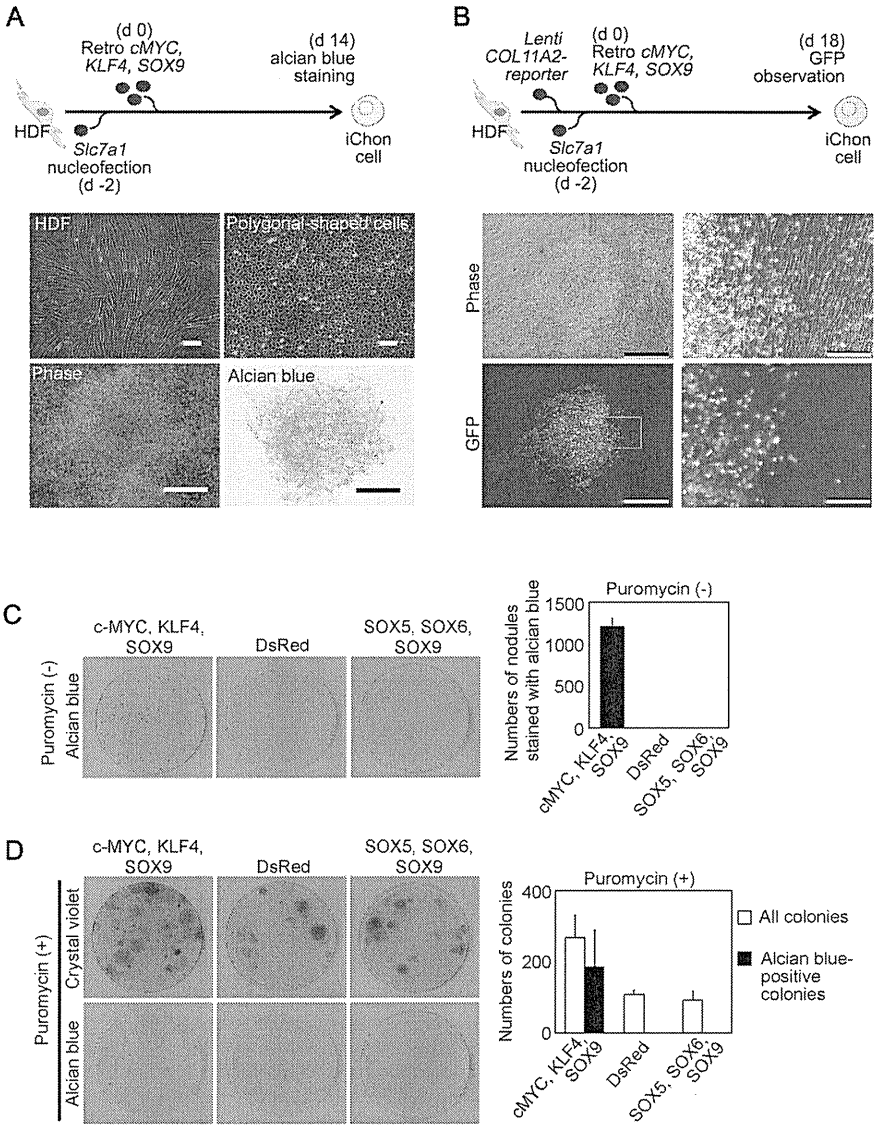

Figure 1. The generation and selection of induced chondrogenic (iChon) cells from human dermal fibroblast (HDF) culture. (**A**) Top, a schematic diagram of the gene transduction. Middle left, HDFs. Middle right, polygonal-shaped cells generated by transduction of c-MYC, KLF4, and SOX9. Bottom left, nodules formed by polygonal-shaped cells. Bottom right, nodules were intensely stained with alcian blue, suggesting the production of glycosaminoglycan. Bars in top panels, 100 μm; Bars in bottom panels, 500 μm. (**B**) Top, a schematic diagram of the gene transduction. Left middle and bottom panels, phase and GFP images of cell nodules formed in HDF culture at 18 days after transduction with c-MYC, KLF4 and SOX9. Right middle and bottom panels, magnification of the boxed region in the left panels. Cells were cultured in the absence of puromycin Bars in left panels, 500 μm; Bars in right panels, 100 μm. (**C**) HDF cultures which had been transduced with lentiviral *COL11A2*- reporter vectors and nucleofected with *Slc7a1* were transduced with retroviral c-MYC, KLF4 and SOX9, or DsRed fluorescent protein, or SOX5, SOX6 and SOX9. Cells were cultured in the absence of puromycin. Dishes (10 cm in diameter) were stained with alcian blue 21 days after retroviral transduction. The numbers of nodules with positive alcian blue staining were counted. (**D**) HDF cultures which had been transduced with lentiviral *COL11A2*- reporter vectors and nucleofected with *Slc7a1* were transduced with retroviral c-MYC, KLF4 and SOX9, or DsRed fluorescent protein, or SOX5, SOX6 and SOX9. Puromycin was added to the medium 7 days after retroviral transduction. Dishes (10 cm in diameter) were stained with crystal violet and alcian blue 21 days after retroviral transduction. The numbers of all colonies stained with crystal violet (white bars) and the numbers of colonies with positive alcian staining (black bars) were counted. In (C and D), after nucleofection of *Slc7a1*, HDFs were replated at a density 5×10^5 cells per 10 cm dish for retroviral transduction. Cells were split 1:5 onto 10 cm dishes immediately after completion of the retroviral transductions. The numbers of nodules in five 10 cm dishes which were derived from one identical dish were added together. Error bars indicate ± SD ($n=3$ dishes).
doi:10.1371/journal.pone.0077365.g001

fibroblast-marker gene *COL1A1* were demethylated in human iChon cells, whereas it was not methylated in the parental HDFs (Figure 3C). These results suggest that the fibroblast marker gene, *COL1A1*, was silenced during the induction of human iChon cells.

We next investigated the cartilage tissue-forming activities of iChon cells by pellet culture. The histology of the pellet culture of iChon cells showed cartilaginous structures (Figure 4A). The matrix of the iChon pellet showed intense metachromatic toluidine blue staining, whereas that of CD-hBMSC pellet looked fibrous. The matrix was hardly formed in the HDF pellet. Picrosirius red staining revealed the fibrous alignment of collagen fibers in CD-hBMSC pellet and HDF pellet, but not in the iChon pellet under polarized microscopic observations. These results suggest that the matrix of the iChon pellet has a hyaline cartilaginous structure;

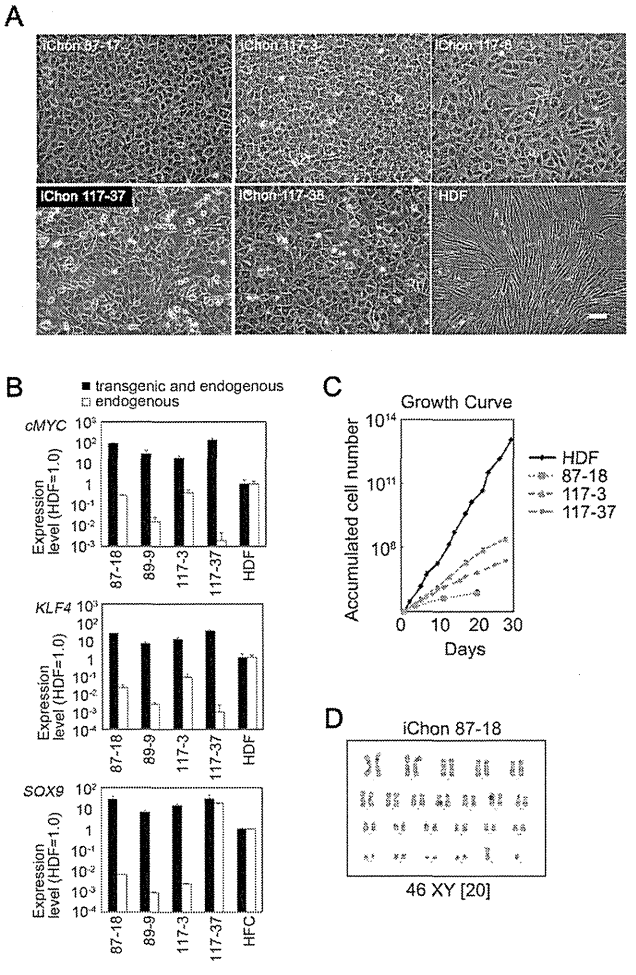

Figure 2. The characteristics of human iChon cell lines. (**A**) Phase images of human iChon cell lines and HDFs. The photos were taken when the cell numbers had expanded and reached 10^7. Bar: 100 μm. (**B**) The mRNA levels of *cMYC*, *KLF4* and *SOX9* in iChon cells. The relative expression levels in comparison to human HDFs or HFCs are shown. The mRNA levels were determined by a real-time RT-PCR analysis using primers specific for endogenous transcripts (white columns) and those common for both transgenic and endogenous transcripts (black columns). The error bars indicate ± SD ($n=3$). (**C**) The growth curves of human iChon cells and parental HDFs. (**D**) The karyotype of human iChon cells. iChon cell line #87-18 was examined at passages 15. A total of 20 cells for each cell line were examined. HDF, human dermal fibroblasts; HFC, redifferentiated human fetal chondrocytes.
doi:10.1371/journal.pone.0077365.g002

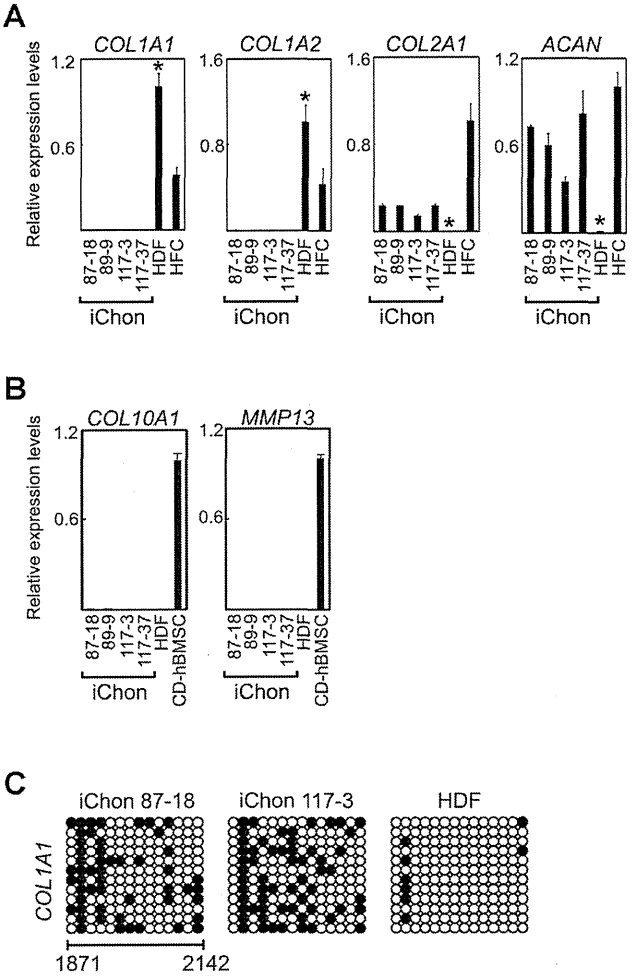

Figure 3. Marker gene expression of human iChon cell lines. RNA samples were extracted from iChon cells at passage 7. (**A**) The quantitative expression analyses of chondrocyte and fibroblast marker genes in human iChon cell lines, HDFs and HFC. Error bars indicate the ± SD ($n=3$). *$P<0.01$ compared with iChon cell lines by Student's t-test. (**B**) The quantitative expression analyses of chondrocyte hypertrophy and terminal differentiation marker genes in human iChon cell lines, HDFs and CD-hBMSCs. Error bars indicate the ± SD ($n=3$). The relative expression levels of *COL10A1* and *MMP13* mRNAs were zero in iChon cell lines. (**C**) Methylation of the regulartory region of the *COL1A1* gene. Bisulfite genomic sequencing of the regulartory regions of *COL1A1* was performed using DNA derived from iChon cell lines and HDFs. Each horizontal row of circles represents an individual sequencing result from one amplicon. Open circles indicate unmethylated CpG dinucleotides, while closed circles indicate methylated CpGs. The nucleotide numbers for *COL1A1* are indicated at the bottom. The ATG translation initiation codon is set as +1 (GenBank accession number NC 000017, nt 48261457). HDFs, human dermal fibroblasts; HFC, redifferentiated human fetal chondrocytes; CD-hBMSCs, chondrogenically differentiated human bone marrow stem cells.
doi:10.1371/journal.pone.0077365.g003

whereas the matrix of the CD-hBMSC pellet has a fibrocartilaginous structure. Immunohistochemistry showed that the matrix contained type II collagen, but not type I collagen (Figures 4B and 4C). These results suggest that human iChon cells produce hyaline cartilage *in vitro*.

The Origin of Induced Chondrogenic Cells in the HDF Culture

To gain insight into the original cell type which gives rise to chondrogenic cells in HDF culture, we performed time-lapse observations of whole wells of a 6-well plate during the induction of chondrogenic cells (Figure 5). *COL11A2-GFP* fluorescence was not observed at 3 days after retroviral c-MYC, KLF4 and SOX9 transduction throughout the whole wells (Figure 5A, left panel). Some cell clusters expressed *COL11A2-GFP* fluorescence at 8 days after transduction (Figure 5A, second panel, arrowheads), and gradually formed nodules, increasing the level of GFP fluorescence. At 14 days after transduction, some nodules (Figure 5A, third panel, arrowheads) specifically expressed *COL11A2-GFP*, while others did not. We retrospectively analyzed 23 nodules of chondrogenic cells which expressed *COL11A2-GFP* and identified their original cells at the start of induction. The cells of origin of all 23 nodules expressing *COL11A2-GFP* did not express GFP at the start of the induction. A close examination revealed that the cells

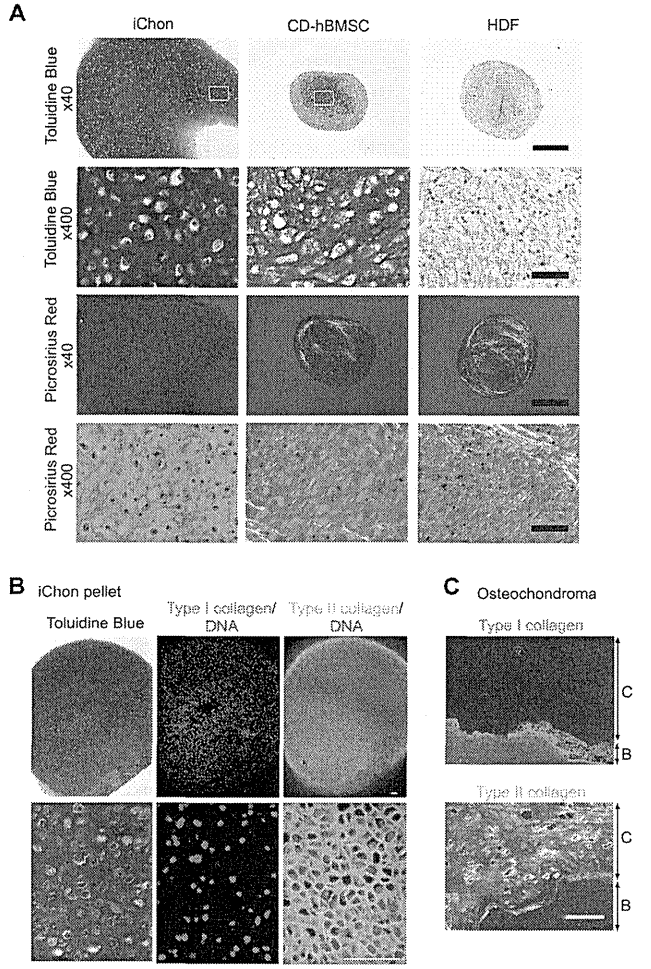

Figure 4. Characterization of matrix of pellet culture of iChon cells. The iChon cells at passage 7 were used. (**A**) After 3 weeks of culture, pellets of iChon cells (# 117-3), chondrogenically differentiated human bone bone marrow stem cells (CD-hBMSC), and human dermal fibroblasts (HDFs) were recovered and processed for histological sections. Semiserial sections were stained with toluidine blue and picrosirius red. Sections stained with picrosirius red were observed under polarized microscopy. Bars in the top and third rows, 500 μm; Bars in the second and bottom rows, 50 μm. (**B**) Semiserial sections of pellets of iChon cells (#117-37) after 3weeks of culture were stained with toluidine blue, and immunostained with anti-type I collagen antibodies and anti-type II collagen antibodies. Bars, 100 μm. (**C**) Control for immunohistological analysis in (B). Histological sections from osteochondroma samples dissected at a time of surgery were immunostained with anti-type I collagen and anti-type II collagen antibodies. Panels are magnification of boxed regions in Figure S7. Bar, 100 μm. *C*, cartilage; *B*, bone.
doi:10.1371/journal.pone.0077365.g004

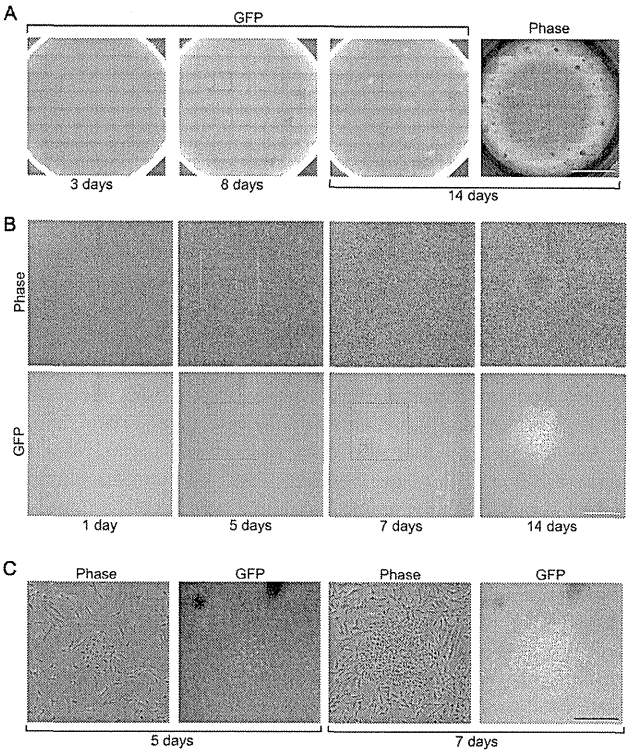

Figure 5. The origins of iChon cells in HDF culture. HDFs were transduced with the lentiviral *COL11A2*-reporter vector, nucleofected with Slc7a1, and transduced with retroviral c-MYC, KLF4 and SOX9 vectors. Cells were replated onto a well of a 6 well plate immediately after completion of the retroviral transduction. The well was cultured in the absence of puromycin and subjected to time-lapse GFP observation using the Biostation CT (Nikon). (**A**) The entire wells were each scanned using a total of 64 images (8 rows×8 columns), and a tiled image was reconstituted. The time-lapse GFP fluorescence of the tiled images at 3, 8 and 14 days after transduction of retroviral c-MYC, KLF4 and SOX9 vectors (3 left panels), and a phase contrast image 14 days after transduction (right panel), spanning an entire well of a 6 well plate are shown. GFP fluorescence was not observed at 3 days after retroviral transduction. Some cell clusters expressed *COL11A2-GFP* fluorescence at 8 days after transduction (arrowheads), and gradually formed nodules, increasing the level of GFP fluorescence. At 14 days after transduction, some nodules (arrowheads) specifically expressed *COL11A2-GFP* and others did not. Bar, 10 mm. (**B**) The magnification of the boxed regions in (A). At 1 day after transduction, no cells expressed *COL11A2-GFP*, suggesting that they were not chondrogenic cells. A cluster of cells with polygonal morphology started to express *COL11A2-GFP* weakly (arrow) at 5 days after transduction. The cells in the cluster increased in number and expressed *COL11A2-GFP* (half-arrow) at 7 days after transduction. A cell cluster formed multiple layers, forming a nodule which expressed *COL11A2-GFP* strongly at 14 days after transduction. These results suggest that iChon cells are derived from non-chondrogenic cells which did not express *COL11A2-GFP*. Bar, 100 μm. (**C**) Magnification of the boxed regions in (B). GFP images were enhanced to detect weak fluorescent signals. Only the polygonal cell clusters expressed *COL11A2-GFP*, but the surrounding fibroblast cells did not express *COL11A2-GFP*. Bar, 50 μm.
doi:10.1371/journal.pone.0077365.g005

from which the *COL11A2-GFP*-positive cells originated did not express *COL11A2-GFP* one day after transduction with c-MYC, KLF4 and SOX9, and only started to express *COL11A2-GFP* at 5–7 days after transduction (Figures 5B and 5C, and Movies S1 and S2). The mouse *Col11a2* regulatory sequences which correspond to the human *COL11A2* promoter-enhancer used in the lentiviral *COL11A2*-reporter gene direct the expression from prechondrogenic cells during mesenchymal condensation [12,16].

In addition, we examined the proportions of cells expressing SOX9 in HDF culture. SOX9 is known to be expressed in chondroprogenitor cells [22]. Immunofluorescence staining of parental HDFs with anti-SOX9 antibodies revealed that the signals were at the background level in almost all cells (Figure S4). The ratio of possible prechondrogenic cells indicated by immunoreactivity against anti-SOX9 antibody in the HDF culture (0.019%, Figure S4C) was lower than the frequency of alcian blue-positive cells generated from HDFs (0.24%, Figure 1D). A close examination revealed that almost all SOX9-positive signals in the

HDF culture were false-positive signals, because the signals were on the edge of cells or debris and did not localize in in the nucleus. These results collectively suggest that non-chondrogenic cells were the major source of the iChon cells.

Hyaline Cartilage Formation by Human iChon Cells in the Subcutaneous Spaces in Nude Mice

We next investigated the cartilage-forming activities of iChon cells *in vivo*. We injected independent iChon cell lines suspended in the medium into the subcutaneous spaces of nude mice (Table S1). Four weeks after injection, we found solid nodules at 14 out of the 42 sites that were injected (33%). We found no nodule formation in the other 28 sites. A histological analysis revealed that these nodules contained cartilage-like tissue (Figure 6A). Cells were scattered in the matrix, which was positively stained with safranin O. We recognized that the cells resided in lacuna, which is characteristic of cartilage histology. An immunohistochemical analysis showed that the matrix contained type II collagen, but not type I collagen, suggesting that the tissue formed by the injection of human iChon cells was hyaline cartilage (Figure 6B). The cells in the cartilage expressed human vimentin, indicating that the injected iChon cells survived and formed cartilage. Longer-term observation showed that the formed cartilage gradually disappeared from the subcutaneous spaces (Table S1). We found no tumor formation at 76 injected sites, including 17 sites that were observed for 3 months (Table S1).

Cartilaginous Tissue Formation by Human iChon Cells in the Articular Cartilage Defects Created in the SCID Rat

We further examined whether iChon cells form cartilage in orthotopic sites. We implanted human iChon cells into defects created in the articular cartilage of six knees of SCID rats. Four weeks after implantation, the defects were partially filled with cartilaginous tissue in four out of the six knees (Figure 6C). The cartilaginous tissues showed positive immunostaining for type II collagen. The expression of type X collagen was below the limit of detection. Immunostaining for human vimentin showed that the cartilaginous tissue was composed of human cells. The human iChon cell-derived cartilaginous tissue was surrounded by scar tissue which consisted of host cells. These results suggest that human iChon cells survive and form cartilaginous tissue in the articular cartilage defects for at least four weeks.

The Low Susceptibility of Human iChon Cells to Osteogenic Conditions

We examined how iChon cells respond to osteogenic conditions. Human iChon cells did not express the OSTEOCALCIN gene (*BGLAP*) or RUNX2 gene when they were cultured in the osteogenic medium containing 100 ng/ml BMP2 for 21 days, although expression of the OSTERIX gene (*SP7*) and the alkaline phosphatase gene (*ALPL*) were slightly increased by the addition of BMP2 (Figure 7A). The *SP7* and *ALPL* genes were expressed in chondrocytes as well as osteoblasts.

Human iChon cells produced cartilaginous tissue and did not form bone, when implanted into the defects created in the calvaria of SCID mice (Figure 7B). The calvarial defects were healed spontaneously, and found to be filled with host bone tissue. These results collectively suggest that human iChon cells did not respond to osteogenic conditions.

Discussion

Although small articular cartilage defects measuring less than 2 cm^2 in size can be treated with autologous chondrocyte transplantation, the treatment of larger cartilage defects remains a challenge. Cell reprogramming techniques have the potential to resolve this problem by providing a sufficient number of hyaline chondrocytes to fill large defects. In this study, we generated human iChon cells directly from HDF culture by transduction of two reprogramming factors (c-MYC and KLF4) and one chondrogenic factor (SOX9). Human iChon cells were generated from non-chondrogenic cells in HDFs, as indicated by the lack of *COL11A2* promoter/enhancer activities and the fact that the majority of the cells had no endogenous SOX9 expression. Human iChon cells generated hyaline cartilage without tumor formation in the subcutaneous space of nude mice. Human iChon cells also formed cartilage in the defects of articular cartilage and did not respond to osteogenic conditions. These results suggest that human iChon cells can be a candidate cell source for regenerative medicine to treat articular cartilage diseases.

It was previously reported that a high level of overexpression of SOX5, SOX6 and SOX9 could activate the expression of chondrocyte-markers in HDFs using adenoviral vectors [11], although fibroblastic characteristics appeared to be remained. We found that the retroviral transduction of c-MYC, KLF4, and SOX9 following *Slc7a1* nucleofection produced substantial numbers of cartilaginous nodules in HDF culture, whereas retroviral transduction of SOX5, SOX6 and SOX9 following *Slc7a1* nucleofection did not. These results indicate that the reprogramming factors c-MYC and KLF4 more efficiently contribute to the SOX9-induced conversion of fibroblasts into chondrogenic cells than SOX5 and SOX6. c-Myc and Klf4 are responsible for erasing the characteristics of fibroblasts during iPS cell induction by c-Myc, Klf4, Oct3/4 and Sox2 [23]. The expression of fibroblast markers was observed to decrease first, followed by an increase in the expression of chondrocyte markers during the induction of mouse chondrogenic cells from MDFs by c-Myc, Klf4 and SOX9 [14]. These findings suggest that c-MYC and KLF4 are involved in epigenetic events in HDFs, and enable SOX9 to direct cells to the chondrogenic lineage during the induction of iChon cells.

The c-MYC, KLF4, and SOX9 transgenes were not silenced in human iChon cells. The silencing of retroviral transgenes is a phenomenon that is a characteristic of pluripotent cells [24] including iPS cells [15]. Retroviral transgenes are not usually silenced in somatic cells and somatic cells which are produced by direct conversion technique [12,25,26]. Human iChon cells expressed neither type X collagen nor MMP13. Human iChon cells retain their chondrogenic phenotype after being passaged in monolayer culture. These results suggest that human iChon cells therefore stay in hyaline chondrocytes and do not undergo hypertrophy. This characteristic of human iChon cells is favorable when considering their application to cell transplantation for the potential treatment of defects of articular cartilage which consists of hyaline cartilage and seldom undergo hypertrophy. CD-hBMSCs tend to undergo hypertrophy and thus can be lost quickly after cell transplantation [27]. Human iChon cells do not undergo hypertrophy, probably because of their continued expression of the SOX9 transgene.

Cell type conversion through iPS cells is associated with two different risks of tumor formation: one is the risk of teratoma formation associated with the pluripotency of iPS cells [28], and the other is associated with the transduction of the reprogramming factors [13]. The iChon cells are theoretically free from the former

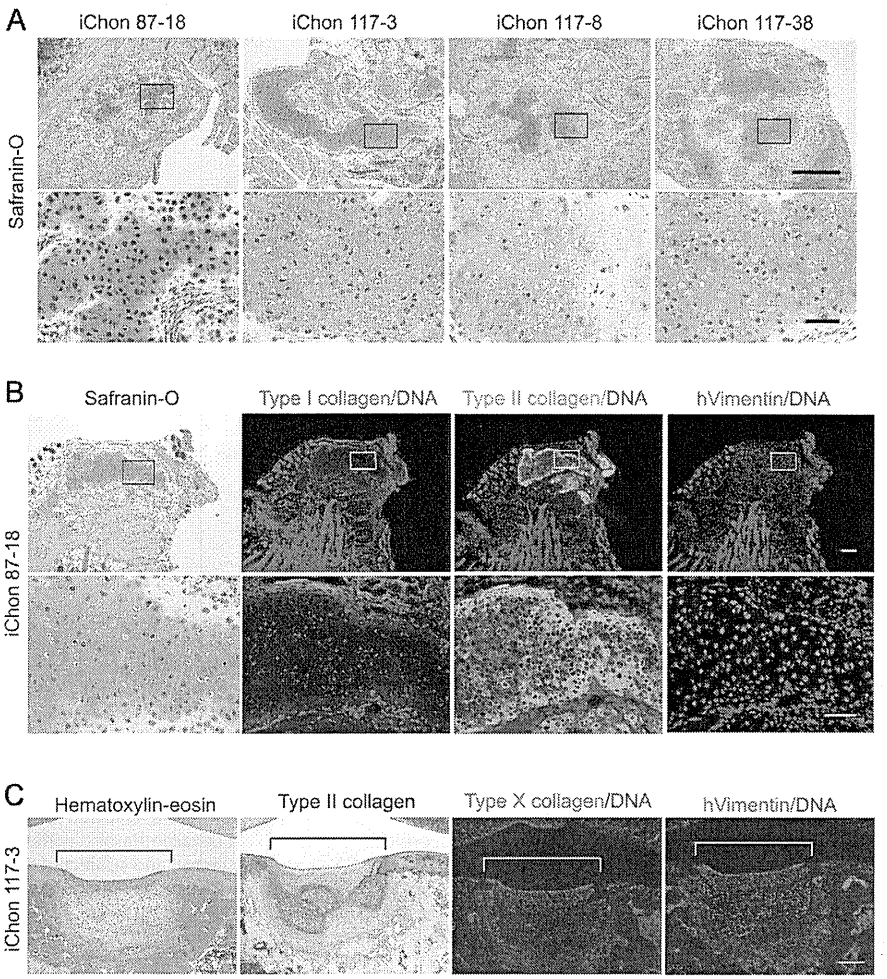

Figure 6. *In vivo* cartilage formation by human iChon cells in the subcutaneous spaces of nude mice (A and B) and articular cartilage defects created in SCID rat (C). The iChon cells at passage 7 were used. Mice were sacrificed at 4 weeks after subcutaneous injection of iChon cells, and nodules at the injected sites were collected. Rats were sacrificed 4 weeks after implantation. (**A**) The histological features of nodules formed by injected iChon cells into subcutaneous spaces of nude mice. Safranin O-fast green-iron hematoxylin staining. Cartilaginous matrix was specifically stained with Safranin O as an orange color. Bars in top panels, 500 μm; Bars in bottom panels, 100 μm. (**B**) The expression of differentiation-related proteins in nodules formed by injected iChon cells into subcutaneous spaces of nude mice. Semiserial sections of nodules derived from injected 87-18 human iChon cell were stained with Safranin O-fast green-iron hematoxylin and immunostained with anti-type I collagen, anti-type II collagen and anti-human vimentin antibodies. The bars in top panels, 500 μm; in bottom panels, 100 μm. (**C**) Human iChon cells (line #117-3) were implanted into defects created in the articular cartilage of the distal femurs of SCID rats. Four weeks after implantation the rats were sacrificed. Semiserial sections were stained with hematoxylin-eosin and immunostained with anti-type II collagen, anti-type X collagen, and anti-human vimentin antibodies. Brackets indicate regions of defects created in the articular cartilage. The bars, 100 μm.
doi:10.1371/journal.pone.0077365.g006

risk, because mouse iChon cells do not enter a pluripotent state during induction, as indicated by the lack of Nanog-GFP expression during induction [14]. However, iChon cells are obviously still associated with the latter risk, because c-MYC and KLF4 are used, although the human iChon cells did not produce tumors for at least 3 months after being injected into nude mice. Safer iPS cells have recently been generated by using integration-free vectors such as episomal plasmid vectors [29] and Sendi virus vectors [30]. Because persistent transgene expression is not necessary for the maintenance of mouse iChon cells as long as they are cultured in a chondrogenic medium containing TGF-β and BMPs [12], it will be ideal to generate human iChon cells by transient expression of c-MYC and KLF4 using integration-free vectors, to minimize the risk of tumor formation. The persistent expression of the SOX9 transgene may positively contribute to the stable chondrogenic phenotype of iChon cells without undergoing hypertrophy in this study. If iChon cells are generated by the transient expression of c-MYC, KLF4 and SOX9, such iChon cells would undergo hypertrophy in a manner similar to that of CD-hBMSCs. An engineered cartilage using CD-hBMSCs undergo hypertrophy faster than articular cartilage and thus can be lost quickly after cell transplantation [27]. However, the constitutive expression of Sox9 can be of another concern, because all tissues undergo remodeling *in vivo*, and an engineered cartilage that does not respond to physiological regulation may present long-term challenges. Further study will thus be needed to stringently control the hypertrophy of such iChon cells during cartilage repair.

Human iChon cells differ from mouse induced chondrogenic cells in several aspects. The karyotypes of the majority of human iChon cells were normal, whereas the karyotypes are fairly unstable in mouse iChon cells [12]. Human iChon cell lines did

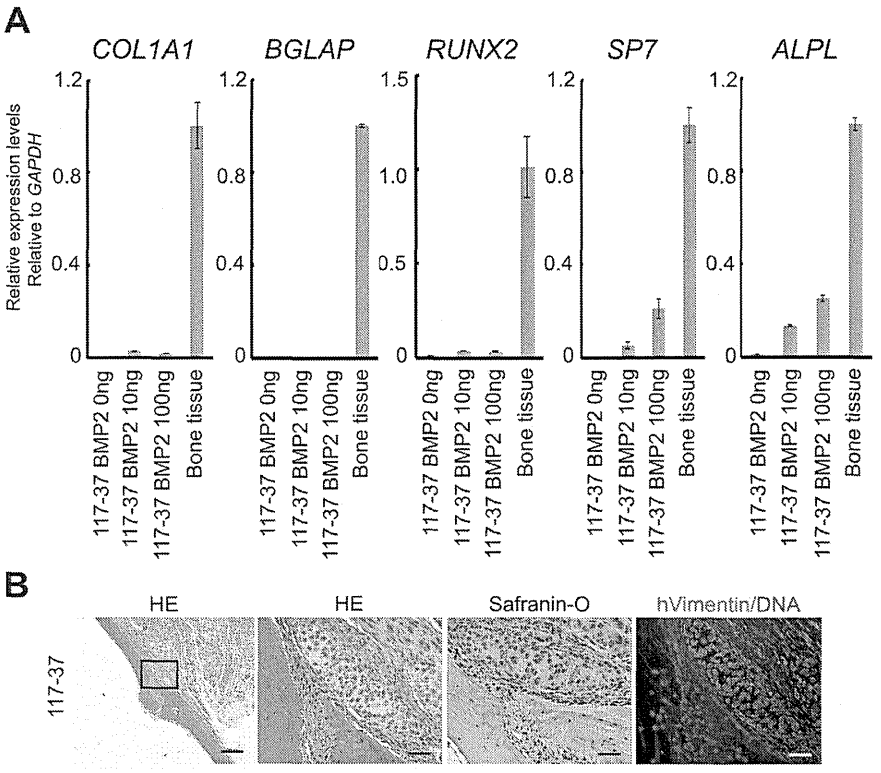

Figure 7. The response of human iChon cells to osteogenic conditions. (**A**) Human iChon cells (line #117-37) were cultured in the osteogenic medium (α-MEM supplemented with 10% FBS, 10 mM β-glycerophosphate, 50 μg/ml ascorbic acid, and 10^{-7} M dexamethasone with the absence or presence of various concentrations of BMP2 as indicated at the bottom of the graphs) for 21 days. RNAs were extracted and subjected to a real-time RT-PCR expression analysis. Error bars indicate the ± SD ($n = 3$). (**B**) Human iChon cells were implanted into defects created in the calvaria of SCID mice. Three weeks after implantation, the mice were sacrificed. Semiserial sections were stained with hematoxylin-eosin and safranin O, and immunostained with anti-human vimentin antibodies. The magnification of boxed regions in the left panel is shown in the right three panels, respectively. The bars in the left panels, 250 μm; in the other panels, 50 μm.
doi:10.1371/journal.pone.0077365.g007

not form tumors when transplanted into nude mice, whereas inappropriately reprogrammed mouse induced chondrogenic cells developed into tumors [12]. A possible reason for the more stable karyotypes and non-tumorigenicity of human iChon cells is related to the limited proliferative activities of human iChon cells, whereas mouse induced chondrogenic cells appear to have almost unlimited proliferative potential [12].

Stable karyotypes and non-tumorigenicity are favorable characteristics of human iChon cells when considering their application to regenerative medicine. Although various obstacles remain, human iChon cells can contribute to the development of cell sources to generate hyaline cartilage-related biomaterials.

Supporting Information

Figure S1 The lentiviral *COL11A2*- reporter vector. (A) A schematic representation of the lentiviral vectors carrying EGFP-IRES-Puro linked to the *COL11A2* promoter plus the *COL11A2* enhancer. (B) *Left*, EGFP expression in human dermal fibroblasts (HDFs) and human chondrosarcoma (HCS-2/8) cells transduced with the lentiviral *COL11A2*-reporter vector. Bars, 100 μm. *Right*, the results of a flow cytometric analysis of the EGFP expression from the reporter vectors in the cells.
(JPG)

Figure S2 An immunoblot analysis of the expression of SOX5, SOX6 and SOX9 retroviral vectors in HDF culture. The Plat-E cells were transfected with pMXs-SOX5, pMXs-SOX6, pMXs-SOX9 and pMXs-EGFP. Supernatants containing each of the retroviruses were added to the HDFs that had been nucleofected with Slc7a1. The cells were lysed 7 days after retroviral transduction, and then were subjected to an immunoblot analysis using anti-SOX5, anti-SOX6 and anti-SOX9 antibodies (Supplementary Table S4) as indicated on the left of membranes (top row). Membranes were reprobed with anti-β-actin antibodies (bottom row).
(JPG)

Figure S3 The presence of transgenes in iChon cells, karyotypes of iChon cells, and marker gene expression in iChon cells after passage numbers. (**A**) The presence of transgenes in iChon cells. PCR reactions were performed with template genomic DNA extracted from each iChon cell line using primers specific for each transgene. GAPDH was used as a control. HDF, human dermal fibroblasts. (**B**) The karyotypes of human iChon cells. iChon cell lines #117-3 and #117-37 were examined at passages 18 and 22, respectively. A total of 20 cells for each cell line were examined. (**C**) The results of an analysis of marker gene expression in iChon cell lines (#89-9 and #117-37) after various passage numbers. *P9*, passage 9; *P11*, passage 11; *P13*, passage 13. The expression levels of chondrocyte markers were maintained, and the expression of fibroblast markers was maintained at low levels, after all of the passage numbers examined. Error bars indicate the ± SD (n = 3 dishes). HDFs, human neonatal dermal fibroblasts; HFCs, redifferentiated human fetal chondrocytes.

(JPG)

Figure S4 The frequencies of prechondrogenic cells in HDF cultures. (A) Immunofluorescence staining of human dermal fibroblasts (HDF) in one well of a 6 well plate with anti-SOX9 antibodies. The nuclei were stained with PI. Each whole well was scanned as an 8×8 image, and the tiling images were reconstituted using the Biostation CT (Nikon). Top left, a tiling image of SOX9 immunofluorescence. Bottom left, magnification of the boxed region in the top left panel. Phase images (top right) and nuclear stained images with PI (bottom right) corresponding to the bottom left panel. Bars in the top left panels, 10 mm; bars in the bottom left, top right and bottom right panels, 100 μm. (B) As a positive control for SOX9 immunofluorescence, mouse induced chondrogenic MK-7 cells (Hiramatsu, et al., *J Clin Invest* 121(2): 640-57) were used. Bar, 100 μm. (C) The frequencies of cells showing immunoreactivity against anti-Sox9 antibodies in HDF culture. The cell numbers were counted with the CL-Quant software program (Nikon). Three wells of a 6-well plate were analyzed. The positive cell numbers represent the numbers of cells showing immunofluorescence (Alexa Fluor) with anti-Sox9 antibodies.
(JPG)

Figure S5 Controls for the immunohistochemical analysis. Histological sections from osteochondroma samples dissected at a time of surgery were immunostained with anti-type I collagen and anti-type II collagen antibodies under the conditions used in this study. The hyaline cartilage of the cartilage cap (arrows) showed immunoreactivity against the anti-type II collagen antibody, but did not show immunoreactivity against the anti-type I collagen antibody. Magnification of boxed regions are shown in Figure 4C. Bar, 1 mm.
(JPG)

Table S1 The results of the subcutaneous injection of human iChon cell lines into nude mice.
(DOC)

Table S2 The sequences of the primers used for the transgenes.
(DOC)

Table S3 The sequences of primers for the marker genes, bisulfite sequencing, and PCR cloning.
(DOC)

Table S4 The antibodies used for the experiments.
(DOC)

Movie S1 Time-lapse images taken during the induction of iChon cells. HDFs were transduced with the lentiviral *COL11A2* reporter vector, nucleofected with *Slc7a1*, and transduced with retroviral c-MYC, KLF4 and SOX9 vectors. Cells were replated onto a well of a 6 well plate immediately after completion of the retroviral transduction. The well was cultured in the absence of puromycin and subjected to time-lapse GFP observation using the Biostation CT program (Nikon). Phase (Movie S1) and GFP (Movie S2) images were captured every 8 h for 14 consecutive days. Each image is shown for 0.5 sec, thus 8 h corresponds to 0.5 sec.
(AVI)

Movie S2 Time-lapse images taken during the induction of iChon cells. HDFs were transduced with the lentiviral *COL11A2* reporter vector, nucleofected with *Slc7a1*, and transduced with retroviral c-MYC, KLF4 and SOX9 vectors. Cells were replated onto a well of a 6 well plate immediately after completion of the retroviral transduction. The well was cultured in the absence of puromycin and subjected to time-lapse GFP observation using the Biostation CT program (Nikon). Phase (Movie S1) and GFP (Movie S2) images were captured every 8 h for 14 consecutive days. Each image is shown for 0.5 sec, thus 8 h corresponds to 0.5 sec.
(AVI)

Acknowledgments

We thank Shinya Yamanaka for providing the vectors. We also thank Toshio Kitamura for the Plat-E cells and pMX retroviral vectors. We are thankful to the National BioResource Project - Rat (http://www.anim.med.kyoto-u.ac.jp/NBR/) for providing rat strains (F344-Il2rgtm2kyo). We thank Shigeyuki Wakitani for articular cartilage defect model of rats and Masaharu Takigawa for human chondrosarcoma cells (HCS-2/8). We thank Kunihiko Hiramatsu, Yoshiki Minegishi, Daisuke Ikegami, Takao Iwai Mari Shinkawa and Miho Morioka for their assistance and discussions. We thank Junya Toguchida and Hidetoshi Sakurai for their critical reading of the manuscript.

Author Contributions

Conceived and designed the experiments: HO MO AY HY NT. Performed the experiments: HO MO AY KN NT. Analyzed the data: HO MO KN HY NT. Contributed reagents/materials/analysis tools: HO MO AY KN HY NT. Wrote the paper: HO NT.

References

1. Frisbie DD, Trotter GW, Powers BE, Rodkey WG, Steadman JR, et al. (1999) Arthroscopic subchondral bone plate microfracture technique augments healing of large chondral defects in the radial carpal bone and medial femoral condyle of horses. Vet Surg 28: 242–255.
2. Bae DK, Yoon KH, Song SJ (2006) Cartilage healing after microfracture in osteoarthritic knees. Arthroscopy 22: 367–374.
3. Bedi A, Feeley BT, Williams RJ III (2010) Management of articular cartilage defects of the knee. J Bone Joint Surg Am 92: 994–1009.
4. Goessler UR, Bugert P, Bieback K, Baisch A, Sadick H, et al. (2004) Expression of collagen and fiber-associated proteins in human septal cartilage during in vitro dedifferentiation. Int J Mol Med 14: 1015–1022.
5. Bi W, Deng JM, Zhang Z, Behringer RR, de Crombrugghe B (1999) Sox9 is required for cartilage formation. Nat Genet 22: 85–89.
6. Akiyama H, Chaboissier MC, Martin JF, Schedl A, de Crombrugghe B (2002) The transcription factor Sox9 has essential roles in successive steps of the chondrocyte differentiation pathway and is required for expression of Sox5 and Sox6. Genes Dev 16: 2813–2828.
7. Lefebvre V, Huang W, Harley VR, Goodfellow PN, de Crombrugghe B (1997) SOX9 is a potent activator of the chondrocyte-specific enhancer of the pro alpha1(II) collagen gene. Mol Cell Biol 17: 2336–2346.
8. Lefebvre V, Li P, de Crombrugghe B (1998) A new long form of Sox5 (L-Sox5), Sox6 and Sox9 are coexpressed in chondrogenesis and cooperatively activate the type II collagen gene. EMBO J 17: 5718–5733.
9. Liu Y, Li H, Tanaka K, Tsumaki N, Yamada Y (2000) Identification of an enhancer sequence within the first intron required for cartilage-specific transcription of the alpha2(XI) collagen gene. J Biol Chem 275: 12712–12718.
10. Han Y, Lefebvre V (2008) L-Sox5 and Sox6 drive expression of the aggrecan gene in cartilage by securing binding of Sox9 to a far-upstream enhancer. Mol Cell Biol 28: 4999–5013.
11. Ikeda T, Kamekura S, Mabuchi A, Kou I, Seki S, et al. (2004) The combination of SOX5, SOX6, and SOX9 (the SOX trio) provides signals sufficient for induction of permanent cartilage. Arthritis Rheum 50: 3561–3573.
12. Hiramatsu K, Sasagawa S, Outani H, Nakagawa K, Yoshikawa H, et al. (2011) Generation of hyaline cartilaginous tissue from mouse adult dermal fibroblast culture by defined factors. Journal of Clinical Investigation 121: 640–657.
13. Okita K, Ichisaka T, Yamanaka S (2007) Generation of germline-competent induced pluripotent stem cells. Nature 448: 313–317.
14. Outani H, Okada M, Hiramatsu K, Yoshikawa H, Tsumaki N (2011) Induction of chondrogenic cells from dermal fibroblast culture by defined factors does not involve a pluripotent state. Biochemical and Biophysical Research Communications 411: 607–612.

15. Takahashi K, Tanabe K, Ohnuki M, Narita M, Ichisaka T, et al. (2007) Induction of pluripotent stem cells from adult human fibroblasts by defined factors. Cell 131: 861–872.
16. Tsumaki N, Kimura T, Matsui Y, Nakata K, Ochi T (1996) Separable cis-regulatory elements that contribute to tissue- and site-specific alpha 2(XI) collagen gene expression in the embryonic mouse cartilage. J Cell Biol 134: 1573–1582.
17. Takigawa M, Tajima K, Pan HO, Enomoto M, Kinoshita A, et al. (1989) Establishment of a clonal human chondrosarcoma cell line with cartilage phenotypes. Cancer Res 49: 3996–4002.
18. Takahashi K, Yamanaka S (2006) Induction of pluripotent stem cells from mouse embryonic and adult fibroblast cultures by defined factors. Cell 126: 663–676.
19. Morita S, Kojima T, Kitamura T (2000) Plat-E: an efficient and stable system for transient packaging of retroviruses. Gene Ther 7: 1063–1066.
20. Mashimo T, Takizawa A, Kobayashi J, Kunihiro Y, Yoshimi K, et al. (2012) Generation and characterization of severe combined immunodeficiency rats. Cell Rep 2: 685–694.
21. Argentin G, Cicchetti R, Nicoletti B (1993) Mouse chondrocytes in monolayer culture. In Vitro Cell Dev Biol Anim 29A: 603–606.
22. Akiyama H, Kim JE, Nakashima K, Balmes G, Iwai N, et al. (2005) Osteo-chondroprogenitor cells are derived from Sox9 expressing precursors. Proc Natl Acad Sci U S A 102: 14665–14670.
23. Sridharan R, Tchieu J, Mason MJ, Yachechko R, Kuoy E, et al. (2009) Role of the murine reprogramming factors in the induction of pluripotency. Cell 136: 364–377.
24. Cherry SR, Biniszkiewicz D, van Parijs L, Baltimore D, Jaenisch R (2000) Retroviral expression in embryonic stem cells and hematopoietic stem cells. Mol Cell Biol 20: 7419–7426.
25. Sekiya S, Suzuki A (2011) Direct conversion of mouse fibroblasts to hepatocyte-like cells by defined factors. Nature 475: 390–393.
26. Ieda M, Fu JD, Delgado-Olguin P, Vedantham V, Hayashi Y, et al. (2010) Direct reprogramming of fibroblasts into functional cardiomyocytes by defined factors. Cell 142: 375–386.
27. Pelttari K, Winter A, Steck E, Goetzke K, Hennig T, et al. (2006) Premature induction of hypertrophy during in vitro chondrogenesis of human mesenchymal stem cells correlates with calcification and vascular invasion after ectopic transplantation in SCID mice. Arthritis Rheum 54: 3254–3266.
28. Wernig M, Zhao JP, Pruszak J, Hedlund E, Fu D, et al. (2008) Neurons derived from reprogrammed fibroblasts functionally integrate into the fetal brain and improve symptoms of rats with Parkinson's disease. Proc Natl Acad Sci U S A 105: 5856–5861.
29. Okita K, Matsumura Y, Sato Y, Okada A, Morizane A, et al. (2011) A more efficient method to generate integration-free human iPS cells. Nat Methods 8: 409–412.
30. Seki T, Yuasa S, Oda M, Egashira T, Yae K, et al. (2010) Generation of induced pluripotent stem cells from human terminally differentiated circulating T cells. Cell Stem Cell 7: 11–14.

J Artif Organs (2013) 16:305–315
DOI 10.1007/s10047-013-0711-7

ORIGINAL ARTICLE

Bone tissue engineering with bone marrow-derived stromal cells integrated with concentrated growth factor in *Rattus norvegicus* calvaria defect model

Hirotsugu Honda · Noriyuki Tamai · Norifumi Naka · Hideki Yoshikawa · Akira Myoui

Received: 25 December 2012 / Accepted: 1 May 2013 / Published online: 23 May 2013

Abstract Concentrated growth factor (CGF) is an autologous leukocyte-rich and platelet-rich fibrin (L-PRF) biomaterial termed "second-generation platelet concentrate". CGF contains autologous osteoinductive platelet growth factors and an osteoconductive fibrin matrix. The purpose of this study was to assess the ability of CGF combined with bone marrow stromal cells (BMSCs) to heal critical-size rat calvaria defects in vivo and to modulate the proliferation and osteogenic differentiation of mesenchymal stem cells (MSCs) in vitro. In the in-vivo study, the CGF group regenerated bone better than the control group, and combined therapy with CGF and BMSCs almost completely repaired critical-size bone defects within 12 weeks after surgery. In the in-vitro study, the CGF extract, at concentrations between 1 and 10 %, promoted proliferation, osteogenic maturation, and mineralization of hTERT-E6/E7 human MSCs in a dose-dependent manner but had an inhibitory effect at higher concentrations. In conclusion, a CGF extract promoted the proliferation, osteogenic maturation, and mineralization of mesenchymal stem cells in vitro, and combination therapy with CGF and BMSCs resulted in excellent healing of critical-size bone defects in vivo.

Keywords Concentrated growth factors · Bone tissue engineering · Rat calvaria defect · Bone marrow stromal cells · hTERT-E6/E7

H. Honda · A. Myoui (✉)
Medical Center for Translational and Clinical Research, Department of Medical Innovation, Osaka University Hospital, 2-15 Yamadaoka, Suita, Osaka 565-0871, Japan
e-mail: myoi@hp-mctr.med.osaka-u.ac.jp

H. Honda
e-mail: hhonda@ort.med.osaka-u.ac.jp

N. Tamai · N. Naka · H. Yoshikawa
Department of Orthopaedics, Graduate School of Medicine, Osaka University, 2-2 Yamadaoka, Suita, Osaka 565-0871, Japan

Introduction

Interest has recently been focused on stem or progenitor cell therapy to replace or repair damaged or lost tissue (because of disease or injury) by tissue engineering. Cell therapy for bone regeneration requires an osteoconductive scaffold and growth factors for osteoinduction. Platelets contain a variety of autologous growth factors, including platelet-derived growth factors (PDGF), transforming growth factors β (TGF-β), vascular endothelial growth factors (VEGF), and insulin-like growth factors (IGF), which are of crucial importance in bone healing. Platelets also secrete fibrinogen, and the extensive cross-linking of fibrin α-chains during clot formation strongly enhances the mesenchymal cell migration essential for tissue regeneration [1–5].

In 1998, Marx et al. [6] found that platelet-rich plasma (PRP), a concentrated preparation of platelets now termed "first-generation platelet concentrate", had a positive effect on bone regeneration and wound healing, for which it functioned as a source of autologous growth factors. Since then, PRP has been widely used in many fields including dentistry, dermatology, orthopedics, cosmetics, and cardiothoracic surgery [7]. In general, this large body of PRP studies demonstrated that PRP stimulates the proliferation and differentiation of fibroblasts, osteoblasts, chondrocytes, and mesenchymal stem cells, although some contradictory

results have been reported [8–10], probably because of the diversity of procedures used to isolate PRP.

Concentrated growth factor (CGF) is an autologous leukocyte-rich and platelet-rich fibrin (L-PRF) biomaterial termed "second-generation platelet concentrate" [11]. (Unlike PRP, CGF is obtained by single centrifugation of venous blood by use of a specially programmed centrifuge [12]). CGF contains autologous osteoinductive growth factors derived from platelets and an osteoconductive fibrin matrix. One of the main differences between CGF and most PRP preparations is that CGF production does not require addition of other reagents, i.e. it does not use anticoagulant during blood harvesting or heterozoic thrombin and calcium chloride for platelet activation and fibrin polymerization. Instead of using these reagents, CGF itself slowly polymerizes during centrifugation in a manner similar to natural polymerization in vivo. Such polymerization is crucial for proper three-dimensional (3D) organization of a fibrin network. A CGF-derived fibrin structure is favorable for cytokine enmeshment and cellular migration (because of the 3D organization of a fibrin network) and slowly releases platelet growth factors for at least 7–10 days [13, 14]. These combined observations suggest that combination therapy of CGF with bone marrow stromal cells (BMSCs) may provide all the necessary features (osteoproductive cells: BMSCs, osteoinductive scaffold: fibrin matrix, osteoconductive growth factors: platelet growth factors) for induction of bone growth and regeneration.

The purpose of this study was to determine the effect of the second-generation platelet concentrate, CGF, on human mesenchymal stem cells (hTERT-E6/E7) [15] in vitro and the feasibility of combined therapy of CGF with BMSCs for bone regeneration in a critical-size rat calvaria-defect model in vivo. Our study revealed that CGF promoted the proliferation, osteogenic maturation, and mineralization of mesenchymal stem cells in vitro, and combination therapy of CGF with BMSCs enabled excellent healing of a critical-size bone defect in vivo.

Materials and methods

CGF preparation

This research was approved by the institute's committee on human research and the protocol was found acceptable by them. The experimental protocol was approved (approval number 09140(758-4)-5, date of approval July 28, 2010) by the Institutional Review Board of Osaka University. For the in-vitro experiments, CGF was prepared from human venous blood obtained from three healthy male volunteers (age range 26–37 years). All subjects enrolled in this research gave informed consent. Venous blood was taken, without anticoagulants, directly into a sterile 10-ml tube and was immediately centrifuged in a special centrifuge device (Medifuge®; Slifadent srl, Sofia, Italy) for 13 min. This centrifuge device used a program with the characteristics: 2,700 rpm 2 min, 2,400 rpm 4 min, 2,700 rpm 4 min, and 3,000 rpm 3 min.

For the in-vivo experiments, donor rats were anesthetized by intramuscular injection of a mixture of midazolam (4 mg/kg), medetomidine (1 mg/kg), and butorphanol (5 mg/kg). Blood was collected, by cardiac puncture, without anticoagulants, into a sterile 10-ml tube and was immediately centrifuged by use of a Medifuge® for 13 min. CGF from rats was prepared in the same way as that from humans.

Preparation of a CGF extract

Immediately after CGF preparation, CGF was transferred into a syringe and was gently compressed in the syringe so that it divided into a solid fibrin membrane and a liquid fraction (CGF extract) (Fig. 1).

Cell culture

Cells of a human mesenchymal stem cell line, hTERT-E6/E7, were provided by Dr Junya Toguchida (Kyoto University, Japan). The cells were grown in α-minimum essential medium (α-MEM; Invitrogen, Carlsbad, CA, USA) supplemented with 1 % antibiotics (penicillin–streptomycin; Invitrogen) and 10 % fetal bovine serum (FBS; Hyclone, Road Logan, UT, USA) (growth medium) at 37 °C under a humidified atmosphere of 5 % CO_2. Before each assay, the hTERT-E6/E7 cells were plated and pretreated in pretreatment medium (α-MEM containing 1 % FBS and 1 % antibiotics) for 12 h, and, after attachment, the medium was changed to differentiation medium (α-MEM containing 1 % FBS, 1 % antibiotics, 50 μM ascorbic acid (Sigma–Aldrich, St Louis, MO, USA), 10 mM β-glycerophosphate (Sigma–Aldrich), and 100 nM dexamethasone (Sigma–Aldrich)). The medium was changed every three days.

In the in-vitro proliferation assay and the differentiation assay, we used the human mesenchymal stem cell line, hTERT-E6/E7 because we assumed that using established cell line might produce stable experimental results, even though we needed to use freshly prepared CGFs from different volunteers in each experiment.

Proliferation assay

hTERT-E6/E7 cells were seeded in 6-well plates at a density of 5.0×10^3 cells/cm^2 in pretreatment medium. After attachment, the pretreatment medium was changed to

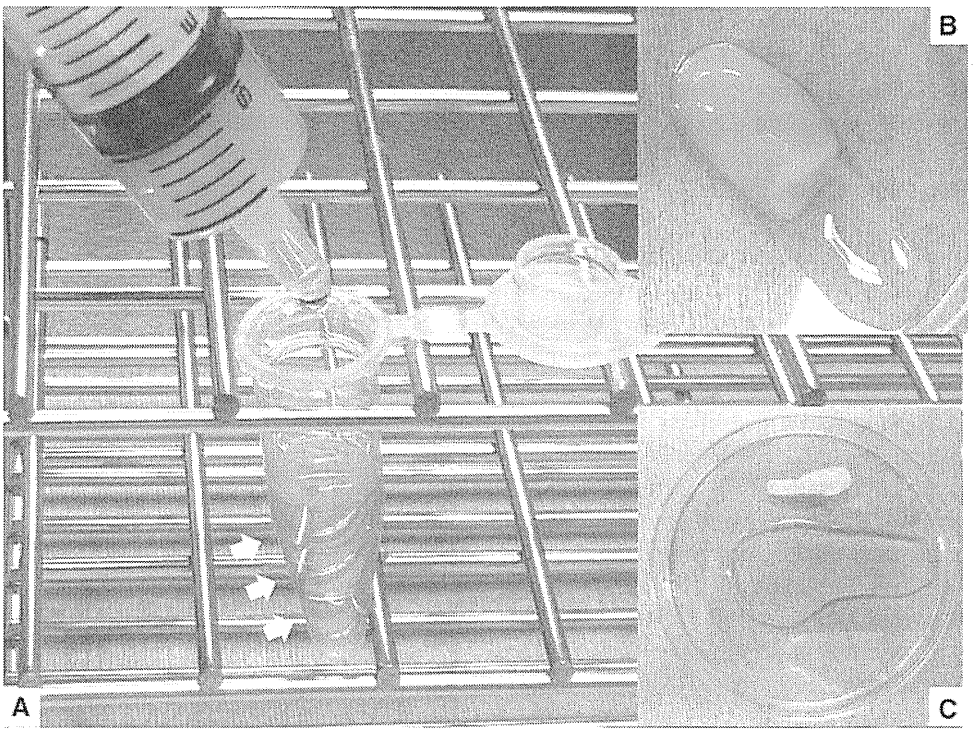

Fig. 1 Preparation of a CGF extract. **a** CGF was transferred into a syringe and was gently compressed in the syringe so that a liquid fraction (the CGF extract is indicated with *white arrows*) was separated from a solid fibrin membrane. **b** CGF **c** solid fibrin membrane (*upper*) and CGF extract (*lower*)

differentiation medium containing 0, 1, 3, 5, 10, or 20 % CGF extract or serum for 24 h. The number of cells was counted after detachment of the cells by use of 0.25 % trypsin EDTA (Invitrogen). All experiments were performed three times, with duplicates.

Alkaline phosphatase (ALP) staining

hTERT-E6/E7 cells were seeded in 24-well plates at a density of 2.0×10^4 cells/cm^2. After incubation for 12 h in pretreatment medium, the medium was changed to differentiation medium containing 0, 1, 3, 5, 10, or 20 % CGF extract or serum for 4 days. For ALP staining, the cells were washed with phosphate-buffered saline (PBS; Sigma–Aldrich) and fixed for 5 min with 10 % formalin at room temperature. After fixing, the cells were incubated with the BCIP/NBT color development substrate (Promega, Madison, WI, USA) for 1 h at 37 °C. After staining, plates were digitally photographed and the acquired images were analyzed.

ALP activity

To measure ALP activity, cells were washed twice with PBS then lysed in mammalian protein extraction reagent (M-PER; Pierce, Rockford, IL, USA) in accordance with the manufacturer's procedure. ALP activity was measured by use of LabAssay ALP (Wako Pure Chemicals Industries, Osaka, Japan) with *p*-nitrophenylphosphate as substrate. To normalize enzyme activity, the protein content of the solution was measured by use of a bicinchoninic acid (BCA) protein assay kit (Pierce).

Alizarin red staining

hTERT-E6/E7 cells were seeded in 24-well plates at a density of 2.0×10^4 cells/cm^2. After incubation for 12 h in pretreatment medium, the medium was changed to differentiation medium containing 0, 1, 3, 5, 10, or 20 % CGF extract or serum for 21 days. The cells were then washed twice with PBS, fixed in 10 % formalin for 10 min, and then stained with alizarin red S (Sigma–Aldrich) at pH 6.3 for 1 h. After discarding the alizarin red S solution and washing the cells three times with distilled water, the bound alizarin red was dissolved in 200 μl 100 mM hexadecylpyridinium chloride (Sigma–Aldrich) and the absorbance of the supernatant was measured at 570 nm.

Von Kossa staining

hTERT-E6/E7 cells were seeded in 24-well plates at a density of 2.0×10^4 cells/cm^2. After incubation for 12 h in pretreatment medium, the medium was changed to differentiation medium containing 0, 1, 3, 5, 10, or 20 % CGF extract or serum for 21 days. The cells were washed twice with PBS, fixed in 10 % formalin for 10 min, then 2 ml freshly prepared 1 % silver nitrate was added to each well and the wells were incubated under UV light for 30 min.

The plates were washed with distilled water, fixed using 5 % sodium thiosulfate for 5 min, then washed thoroughly with distilled water to terminate the reaction. Macro photographs of mineral deposits were then recorded.

Quantitative real-time PCR

Total RNA was isolated from cells by use of the RNeasy mini Kit (Qiagen, Valencia, CA, USA), in accordance with the manufacturer's instructions. cDNA was synthesized by use of the SuperScript III First-Strand synthesis system (Invitrogen). This cDNA was then analyzed by real-time PCR analysis by use of the 7900HT fast real-time PCR system (Applied Biosystems, Tokyo, Japan). The SYBR green assay with SYBR Premix EX taq (Tli RnaseH plus; TaKaRa Bio, Otsu, Japan) was used for amplification of all target transcripts. Expression values were normalized to GAPDH. The sequences of the specific primers used are shown in Table 1.

Measurement of platelet growth factor (PDGF-BB, TGF-β1, TNF-α, IL-1β) levels in CGF CGF, PRP (2,400 rpm 10 min, 3,600 rpm 15 min), and serum were assayed for typical growth factors using commercially available Quantikine ELISA kits (R&D Systems, Minneapolis, MN, USA). We incubated CGF in centrifuge tubes containing 1,000 μl PBS and stored for 13 days at 37 °C. The PBS in the tubes was replaced every 2 days and collected for ELISA.

BMSC isolation and culture

Bone marrow cells were obtained by flushing the bone marrow cavity of rat femoral and tibial bones with 5 ml saline. For BMSC isolation and expansion, the flushed bone marrow fluid was first passed through 90-μm pore strainers for isolation of bone spicules. Next, filtrates containing bone marrow cells were plated in a plastic culture dish in growth medium that had been screened for optimum BMSC growth. After incubation for 24 h, non-adherent cells were removed by means of 2 or 3 PBS washing steps. After 2–3 weeks of culture in this growth medium, the adherent cells were used as BMSCs for in-vivo assays.

Preparation of CGF with BMSCs

BMSCs (5.0×10^5) suspended in 20 μl PBS were injected into CGF (average weight 39.1 ± 1.99 mg) by use of a 1-ml syringe with a 26-gauge needle.

The rat calvaria critical-size bone defect model

Twenty-seven male Sprague–Dawley (SD) albino rats (10–12 weeks old, average weight 300–350 g) were randomly divided into three groups:

1. unfilled defect (control);
2. CGF alone; and
3. CGF + BMSCs.

All animals were housed in cages with free access to food pellets and water. The experimental protocol was approved (Approval Number 21-063-0) by the Animal Experiment Committee of Osaka University, and the experiments were carried out in accordance with the Osaka University guidelines for the care and use of laboratory animals. All efforts were made to minimize suffering. General anesthesia was induced by intramuscular injection of a mixture of midazolam, medetomidine, and butorphanol. An incision was made midline from the supraorbital glabella to the occiput. This incision was continued through the periosteum, which was elevated from the underlying bone and retracted laterally. Two calvarial defects, 5 mm in diameter, were created symmetrically on the bilateral sides of the midline in each rat by use of a trephine bur

Table 1 Sequences of the primers used for quantitative real-time PCR

Gene	Product size	Primer	Sequences(5′ → 3′)
RUNX2	96	Forward	TCCAACCCACGAATGCACTATC
		Reverse	TGGCTTTGGGAAGAGCCG
OSX	92	Forward	GCTGCGGCAAGGTGTAT
		Reverse	GAAGAGCCAGTTGCAGACG
ALP	91	Forward	GAGATACAAGCACTCCCACTTCAT
		Reverse	TGTTCCTGTTCAGCTCGTACT
OPN	88	Forward	CCCATCTCAGAAGCAGAATCTCCTA
		Reverse	ATCATCCATATCATCCATGTGGTCA
COL1A1	86	Forward	AGGGCCTAAGGGTGACAG
		Reverse	GGCCAGTCAGACCACGGA
GAPDH	96	Forward	TCAATGGAAATCCCATCACCATCTT
		Reverse	CGCCAGTGGACTCCACGA

RUNX2 runt-related transcription factor 2, *OSX* osterix, *ALP* alkaline phosphatase, *OPN* osteopontin, *COL1A1* typel collagen alpha 1, *GAPDH* glyceraldehyde 3-phosphate dehydrogenase

without dura perforation. A sterile saline solution was used to keep membranes moist and to thoroughly remove bone debris. The CGF ± BMSCs were applied directly into the defect sites. The skin was closed with 5–0 nylon.

Microfocus computed tomography

Formation of new bone in each calvaria sample was evaluated by use of a microfocus computed tomography (micro-CT) system (SMX-100CT-SV; Shimadzu, Kyoto, Japan). Each sample was scanned at 50-μm intervals at 30 kV and 175 μA. After scanning, 3D CT images were reconstructed and the calcified volume of newly formed bone in the calvarial defect was measured by use of Tri/3D Bon software (Ratoc System Engineering, Tokyo, Japan).

Histological analysis

Samples were fixed in 10 % neutral formalin and were decalcified with ethylenediaminetetraacetic acid (pH 7.4). After decalcification, the samples were dehydrated in a graded ethanol series, cut along the coronal plane at the midline of the defect, and embedded in paraffin. Sections (3 μm thick) were each mounted on to individual slides and stained with H&E for observation under a light and polarized light microscope (Eclipse 90i; Nikon, Tokyo, Japan).

Statistical analysis

All data are expressed as mean ± SD and a minimum of three independent experiments were performed for each assay. A two-sided unpaired Student's *t* test or analysis of variance (ANOVA) followed by Tukey's test for multiple comparisons were used for statistical analysis of differences between groups. A statistical difference between experimental groups was regarded as significant when the *p* value was <0.05.

Results

Quantitative real-time PCR analysis of the effect of CGF extracts on expression of osteoblast-related genes

hTERT-E6/E7 cells were treated with CGF extract at concentrations of 1, 3, 5, 10, or 20 % in the culture medium for 3 days and CGF effects on osteoblastic gene expression were assessed by use of quantitative real-time PCR. Gene expression of ALP and osteopontin (OPN) was significantly increased by treatment with CGF extract (5–20 and 5–10 %, respectively) compared with treatment with the same concentration of serum (Fig. 2). Gene expression of Type 1 collagen alpha 1 (COL1A1) was also increased by treatment with 3–5 % CGF extract, but a high

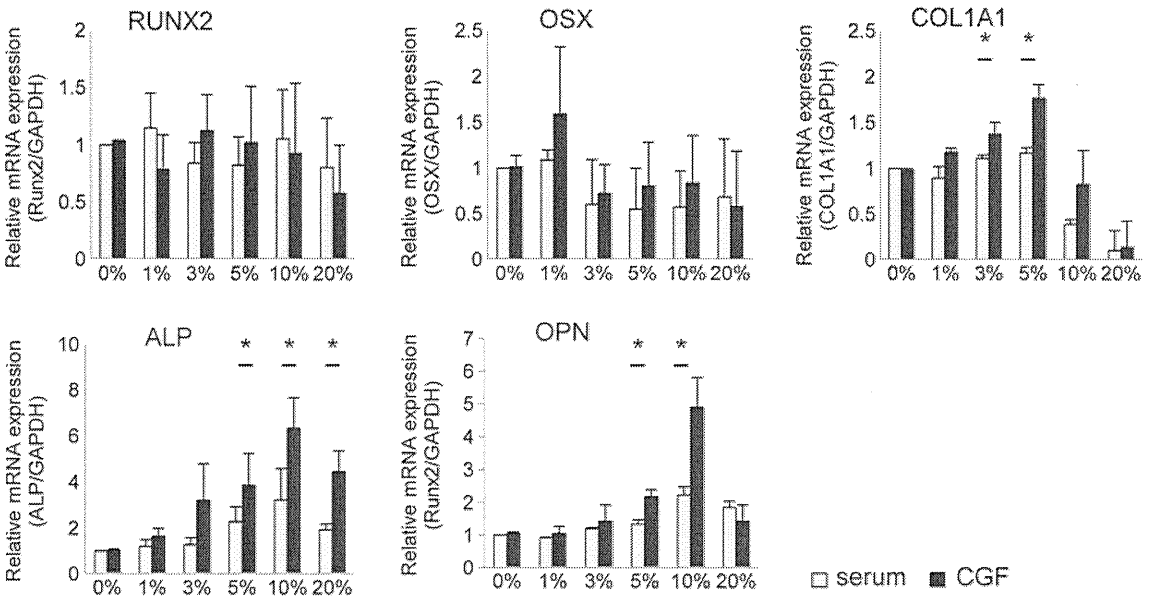

Fig. 2 Quantitative real-time PCR analysis of the effect of CGF extract on expression of osteoblast-related genes. Cells of the human mesenchymal stem cell line hTERT-E6/E7 were treated with different concentrations of a concentrated growth factors (CGF) extract or serum control for 3 days and mRNA expression of the indicated genes was evaluated by use of quantitative RT-PCR. Expression of each gene was normalized to GAPDH expression. All data are mean ± SD from three independent experiments (each experiment used CGF from a different volunteer), each performed in duplicate. (*$P < 0.05$ compared with the serum group of the same concentration.)